ISTANBUL TECHNICAL UNIVERSITY ★ GRADUATE SCHOOL OF SCIENCE ENGINEERING AND TECHNOLOGY

IMPLEMENTATION OF KNN, MLP, PCA ALGORITHMS ON CORTEX-M4 BASED EMBEDDED SYSTEM FOR ENOSE APPLICATION

M.Sc. THESIS

Leila GHORBANI

Department of Mechatronic Engineering

Mechatronic Program

Thesis Advisor: Prof. Dr. Mustak E.YALCIN

JUNE 2014

ISTANBUL TECHNICAL UNIVERSITY ★ GRADUATE SCHOOL OF SCIENCE ENGINEERING AND TECHNOLOGY

IMPLEMENTATION OF KNN, MLP, PCA ALGORITHMS ON CORTEX-M4 BASED EMBEDDED SYSTEM FOR ENOSE APPLICATION

M.Sc. THESIS

Leila GHORBANI
(518101060)

Department of Mechatronic Engineering

Mechatronic Program

Thesis Advisor: Prof. Dr. Mustak E. YALCIN

JUNE 2014

Leila Ghorbani, a **M.Sc.** student of ITU **Institute of / Graduate School of Mechatronic Eng.** student ID 518101060, successfully defended the **thesis** entitled "**IMPLEMENTATION OF KNN, MLP, PCA ALGORITHS ON CORTEX-M4 BASED EMBEDDED SYSTEM FOR ENOSE APPLICATION**", which she prepared after fulfilling the requirements specified in the associated legislations, before the jury whose signatures are below.

Thesis Advisor :	**Prof. Dr. Mustak E. YALCIN**
	İstanbul Technical University
Jury Members :	**Prof. Dr. Osman KAAN EROL**
	İstanbul Technical University
	Assistant Prof. Dr. Yaprak YALCIN
	İstanbul Technical University

Date of Submission: **02 MAY 2014**
Date of Defense: **13 JUNE 2014**

To my family,

FOREWORD

I would like to express my deepest gratitude to all those who made my thesis possible. I am especially grateful for my thesis advisor, Prof. Dr. Mustak E. YALCIN, who supports me with suggestion and advices during thesis.

JUNE 2014 Leila GHORBANI

TABLE OF CONTENTS

Page

ABBREVIATIONS

ADC : Analogue to Digital Convertor
AHB : Advanced High Performance Bus
APB : Advanced Peripheral Bus
API : Application Programming Interface
CAN : Controller Area Network
CPU : Central Processing Unit
DMA : Direct Memory Access
DSP : Digital Signal Processor
GPIB : General Purpose Interface Bus
GPIO : General Purpose Input / Outputs
HIS : High Speed Internal
HSE : High Speed External
I²Cs : Inter-Integrated Circuit
I/O : Input/ Output
LED : Light-Emitting Diode
LSE : Low Speed External
MCU : MICROCONTROLLER
PCLK1 : Internal APB1 clock
PCLK2 : Internal APB2 clock
PLL : Phase Locked Loop
PLLCLK : PLL Clock
PWM : Pulse Width Modulation
RAM : Random Access Memory
RS-232 : A standard for computer serial ports
RTC : Real Time Clock
SRAM : Static Random Access Memory
SPI : Serial Peripheral Interface
SYSCLK : System Clock Source
TIMx : General Purpose and Advanced Control Timers
HVAC : Heating, Ventilation, and Air Conditioning
NN : Neural Network
SVM : Support Vector Machine
K-NN : K Nearest Neighbor
PCA : Principle Component Analysis
LDA : Linear Discriminate Analysis
PPM : Parts Per Million

LIST OF TABLES

Page

LIST OF FIGURES

Page

IMPLEMENTATION OF KNN, MLP, PCA ALGORITHMS ON CORTEX-M4 BASED EMBEDDED SYSTEM FOR ENOSE APPLICATION

SUMMARY

Electronic noses are popular devices nowadays; various applications can be defined for them. They are used in different context like Automotive, Food safety, Telemedicine, Emergency Response , Military and Space, Environmental monitoring. The goal in this thesis is designing an intelligence system that is able to detect odor and have capability to be attached on mobile robot to tracking odors. This robot can be used in security or mining applications. Any gas leakage or emission can be distinguished by the system. The system is composed of two important parts. The first part is sensing part which consists of four Figaro gas sensors is used as a sensor array. Data from sensing part then is transferred to microcontroller. ADC of microcontroller convert analog signal to digital form. These data then is used in the second part of the system that is analyzing part. In this part three algorithms have been used to analyze sensor data.

The first algorithm which is implemented on the system is K Nearest Neighbor (K-NN) algorithms. This algorithm shows good level of performance. Second algorithm is implementation of Multi Layer Perceptron (MLP), we first train system by samples and then new data is given to the algorithm. Using complex and capability of MLP algorithm enables us to analyze data precisely. Database for the training is extracted from datasheet of the sensors. This information then is given to Matlab program, and training be done offline. Weights that are achieved from training are used in Multi Layer Perceptron (MLP) algorithm. According to graphs of datasheet, the ethanol gas has been selected as reference gas, and dataset have been generated based on this gas. Third algorithm that be applied on system is Principle Component Analysis (PCA). PCA algorithm is used to extract feature of system then the outcome can be used by other algorithms. In this thesis, the result of PCA is used in KNN algorithm.

The main purposes of this work is the implementations of the algorithms on embedded system. In this thesis STM32F407 series embedded system which includes a Cortex™-M4 microcontroller is chosen. The algorithms have been implemented on this embedded system which is ready to integrate a mobile robot. The implemented algorithms on the embedded system are alerted the existence of the trained gases and measured the value of the interested gases.

ELEKTRONİK BURUN UYGULAMASI İÇİN MLP, PCA ve KNN ALGORITMALARININ CORTEX M4 TABANLI BİR GÖMÜLÜ SİSTEM ÜZERİNDE GERÇEKLEMELERİ

ÖZET

Elektronik burunlar farklı uygulama alanlarına sahip olan ve gittikçe popülerliği artan cihazlardır. Otomotiv, gıda güvenliği, biyomedikal, güvenlik, savunma ve uzay uygulamaları yanında çevre takibi gibi farklı uygulamalarda da kullanılmaktadırlar.

Elektronik burunlar üzerine yapılan ilk çalışmaların çoğu MOS sensör dizilerinin yapılandırılmasında en baskın teknolojidir. Figaro mühendislik şirketi N.Taguchi tarafından üretilen MOS sensörler bu alanda en büyük üreticilerinden biridir. Sistem iki önemli parçanın birleşiminden oluşmaktadır. İlk kısım sensör dizi kısmı olarak 4 figaro gaz sensörünü içeren algılama kısmıdır. Bu gaz sensörleri de TGS 2600, 2602, 2610, 2620 dir.

TGS sensördeki algılama malzemesi metal oksittir, en tipiği SNO2 , SNO2 gibi bir metal oksit belirli bir sıcaklıkta ısıtıldığında, oksijen negatif yüklü kristal yüzeyde emilir. Tanecik sınırında oksijen emilir ve sonuç olarak potansiyel sınır şekillenir. Bu potansiyel sınırın büyüklüğü; sensörün direnci, sınırların yüksekliği ve sensörlerin çevresindeki direncinde değerinde yansıtılır. Dioksit gaza maruz kalma tanecik sınırını tüketir ve böylece elektrik yükü daha serbest bir şekilde akarak toplam direnç düşer.

Normal şartlar altında herbir sensör fiziksel algılayıcı malzemelerin fabrikasyonlarıyla belirlenen optimize edilmiş bir gaza en yüksek duyarlılıkta pekçok dioksit gaza hassastır.

TGS 2600 sigara dumanında bulunan hidrojen ve karbonmonoksit gibi hava kirletici gazların düşük konsatrasyonuna daha duyarlıdır. Yalnızca TGS 2602 sigara dumanından çıkan hava kirleticilere duyarlı değildir. Ayrıca ev ve ofislerdeki atık maddelerden üretilen ammonia gibi koku gazlarının düşük konsatrasyonlarıda buna dahildir. Diğer bir çeşit ise çok fazla güç tüketmeyen ve uzun ömürlü LP gazına fazla duyarlı yarı iletken tipte bir gaz sensörü olan TGS2610'dur. Bir diğeri ise diğer uçucu buharlara ek olarak organik çözücülerin buharlarına da duyarlı TGS2620'dir. Hem bu model, karbondioksit gibi sıkıştırılabilir gazların değişkenliğine duyarlı olması nedeniyle iyi bir genel amaç sensörü olarak tanımlanır. Ancak sensörlerin birkaç dezavantajı yüksek güç harcama ve gaza ulaşma oranını etkileyen sıcaklık ve harici nem arası ilişkiye dayanır.

Figaro'nun yukarıda bahsettiği gaz sensör serileri ve STM32 F407 mikrokontrolcülerde algılama ve anaaliz kısmı beraber birleştirilir. Bu çalışmadaki ana amaç gömülü sistemlerde algoritmanın gerçekleştirilmesidir. Tezde bir Cortex-M4 mikrokontrol içeren STM32F407 gömülü sistemi seçildi. Cortex-M4 32 bit

çekirdek 168 Mhz frekansa kadar işlem yapan işlemci sinyal işleme ve kompleks algoritmaları uygulama için DSP setini destekler. Pekçok farklı seçenek içerisinden STM32F4 keşif kiti kullanıldı. Bahsedilen keşif kiti için yazılım olarak MKD-ARM kullanıldı.

Gömülü sistemlerde kullanılan bu algoritma mobil bir robota entegre edilmeye hazırdır. Elektronik bir burundan data analizindeki en büyük problem sınırsız değişken seti (n sensör çıkışı) ve sınırlı değişken seti (koku sınıfı) arasında var olan ilişkiden kaynaklanır. Bu bölümde 3 algoritma sensör datalarını analiz etmekte kullanıldı. Algoritmanın 2'si istatiksel yaklaşım değeri iken diğeri biyolojik yaklaşımı temel alır. (İnsan algoritma sürecine benzer bir yaklaşım)

Dataseti, pattern analizi ve algoritması için gereklidir. Veritabanı elde etmek için kullandığımız bu yaklaşım sensörlerin teknik veritablosuna denk gelmektedir ve ham veriyi çıkartır. Bu metodu kullanmaktaki amaç verilen giriş gazına sensör çıkışının doğru bilgiiiyi veren ölçüm aleti eksikliğidir. Veri tablosunda giriş gaz değerleri Rs/Ro değer gösterir. Bu grafikleri kullanarak giriş değer ile sensör çıkış değerleri arasındaki ilişkiyi çıkarım yaparız.

Sistem üzerine uuygulanan ilk algoritma K'nıncı yakın komşuluk (KNN) algoritmasıdır. K'nıncı komşu algoritma; veri havuzu, istatiksel çift tanımlama gibi pekçok alanda akıllı öğrenmenin bir parçasıdır. KNN, özel bir uzayda en yakın eğitilmiş örnek tabanlı objeleri sınıflandırma metodudur. Diğer bir deyişle KNN algoritması farklı bir konsept temellidir. Bu tezde algoritmayı linear kabul ediyoruz. Aardından giriş değerler ile uygulana çıkış değerleri arasındaki farkı hesaplayarak algoritamyı çalıştırırız. Sonuçta mikrokontrolcüden elde edilen çıkış değeri veritablosunda 2 sayının arasında ise girişler arası uzaklığı hesaplar ve bu değeri veritablosunun çıkış değerine yazarız. Cevap gözönüne alınan çıkıştır.

İkinci algoritma çok katlı algılayıcıların gerçekleştirilmesidir. Çok katmanlı bir algılama, birtakım giriş datalarıyla birtakım uygun çıkışları eşleştiren ileri besleme sinir ağları modelidir. MLP akıllı öğrenme fazına sahiptir. Düzenli bir MLP mimarisi giriş, saklı ve çıkış fazı olmak üzere 3 farklı nöron grubundan oluşur. Nöron içeren bölümler saklı ve çıkış kısmındadır. Ve böylece bir NLP 2 katmanın ağırlığı altındadır. Giriş düğümlerinin sayısı tipik olarak dizindeki sensör sayısıyla uyumlu olarak belirlenir. Bu çalışmada sensörden 4 giriş değeri alırız. Saklı katmandaki nöronların sayısı deney yoluyla belirlenir. 2 saklı katmanı seçeriz. Ve bu tezde herbir sensör için 1 çıkış tanımlanır.

Öncelikle örneklerden sistemi deneriz ve sonra algoritmaya yeni data verilir. MLP algoritması kullanmamız bize hasssas data analizi yapmamıza imkan verir. Eğitme için veritabanı sensörlerin veritablolarından çıkarılır. Bu bilgi sonraları MATLAB'a verilir. Matlab sinir ağı araç kutusu eğitim sisteminde kullanılır. Basit ve kullanım kolaylığı olan sinir ağı grafik kullanıcı arayüzü kullanılır. Veritablosunun grafiklerine göre etonol gaz referans gaz olarak seçilir ve veriseti bu gaz temelli üretilir.

Sistem üzerine uygulanan 3. Algoritma temel bileşen analizidir. Datadaki çiftlerin tanımlanıp onların benzerlik ve farklılıklarının analiz edilmesini ifade eden bir yoldur. Bu varyans ve kovaryans konsepti üzerinden yapılır.

PCA bir başka deyişle 1. Koordinata oturan en büyük varyanslı parçayı yeni koordinata dönüştüren bir linear dönüşüm yöntemidir. Bu algoritma data analizi için güçlü bir araçtır. PCA'nın bir başka avantajı datadaki çiftleri bulduğumuz zaman

bilgi ve boyut kaybı olmadan data sıkıştırılabilir. Böylece giriş data sayısı arttığı zaman ve sistemin özelliği ayıklandığı zaman daha popüler olur. Ve böylece sonuşlar diğer algoritmalar tarafından kullanılır. Bu tezde PCA'nın sonucu KNN algoritmasında kullanılır.

Bu işteki teknoloji harikası şey gömülü sistemlerde çalışması ve tüm işlemci kısımlarının taşınabilir mikrokontrolcüler tarafından yapılmış olmasıdır. Bu nokta robot teknolojisinde sistemi kullanmak için bize iman sağlamaktadır. Robotların bu çeşidi gaz kaçağını veya herhangi bir kokuyu bulmak için havaalanları yada petrol rafineleri gibi hassas yerlerde kullanılabilir. Bu tezde algoritma için kullanılan uygulama PPM ölçek tarafından gazın tam değerini ayırt edilmesidir.

1. INTRODUCTION

In the past, odor was considered as only one of the human senses. With the rapid developments in science and technology, people found other applications for smell. Then as there are some limitations to human olfactory system, the need for machine olfactory system was emerged. The ability to artificially imitate the biological sense of smell has been a topic of interest for several decades. New developments in sensor technology has helped enormously achieve necessary requirements. Nowadays, gas sensor has been developing vastly, and is used to detect various gases like carbon dioxide, carbon monoxide, ethanol, methane and oxygen. New technologies of gas sensors combined with pattern recognition techniques and devices that are called electronic noses have been attained. An electronic nose is an instrument that can mimic human olfactory system. The invention of many new e-nose sensor types and arrays based upon different detection principles and mechanisms, is closely correlated with the expansion of new applications. Electronic noses have provided benefits to a variety of commercial industries, including agricultural, biomedical, cosmetics, environmental, food, manufacturing, military, pharmaceutical, regulatory, and various scientific research fields. Advances have improved product attributes, uniformity, and consistency as a result of increases in quality control capabilities which have been afforded by electronic-nose monitoring of all phases of industrial manufacturing processes. The main objective of this thesis is to design an embedded system, which can detect gases precisely by applying Figaro gas sensor and algorithms. The significant point in this thesis is that the system works based on embedment. Therefore, it can be attached on mobile robot for tracking special kind of odor. Afterwards, various applications can be defined for this device. For instance, it can be used in mining exploration. The system can detect dangerous gases and

prevent any explosion. Another application is in refinery stations. The system can detect any leakage of hazardous gases. Some other applications for this system can be at the

airports or places where security is an important factor. This device can be used to detect any gas bomb or other dangerous situation.

1.1 Objective

Studies on electronic olfaction can be separated into two aspects. One deals with the development and improvement of gas sensing technologies. This development is not within the scope of the work presented here. Instead, our main contributions pertain to the second research direction which deals with the integration of electronic olfaction to a number of existing domains. Such domains include medical diagnosis for detection of illness, environmental monitoring, quality evaluation for the foodstuff industry, and mobile robotics. In this thesis, the main focus is on the latter domain concerning the integration of e-noses on robotic platforms. Most applications for olfaction on robotic platforms have focused on the use of gas sensors in mobile robotics for the investigation of odor-based navigation strategies. Yet, the integration of a complex odor recognition component with today's and tomorrow's robotics and intelligent systems offers a growing number of potential applications. A robot with the ability of discriminating odors could be used in a production line, testing the quality of products. The main purpose is to extend olfactory information from a low-level representation to a high-level one, in other words from sensor data to meaningful odor categories. This thesis is primarily concerned with the integration of odor recognition using electronic noses into intelligent systems. In this work, Figaro gas sensors and STM32F407 microcontroller series are combined together in order to provide sensing and analyzing part. Then some algorithms explained later in chapter 2 are applied to the system for classification and clustering of odors and data. A state-of-the-art point in the current work is that it works embedded and all the processing parts are accomplished by microcontroller. The review of important parts of the project will be discussed in this section.

1.2 STM32F407

The following part describes the work precisely in order give more information regarding project operation. The microcontroller STM32F407 receives an Analogue

signal from signal generator. The ADC (Analogue to Digital Convertor) converts the input analogue signal to the Digital Samples (making digital samples of analogue signal). Then the pattern recognition analysis and algorithms be applied on samples. Then the result is displayed on LCD.

1.3 Figaro Gas Sensors

The Figaro Gas Sensor is a gas sensitive semiconductor which was developed by Naoyoshi Taguchi. The Taguchi Gas Sensor (TGS) is a sintered n-type semiconductor bulk device. Most TGS sensors are composed of sintered tin dioxide whose resistance in fresh air is very high and drops dramatically in the presence of reducing gases such as combustibles (methane, propane, CO, hydrogen, etc.), volatile organic vapors (alcohol, ketone, esters, benzols, etc.), and many others.

Figure 1.1: Figaro TGS 2600 gas sensor [14].

These sensors are prominently featured in gas detection equipment throughout the world in the fields of safety, health, control systems, and instrumentation. Popular applications of Figaro Gas Sensors include residential and commercial/ industrial alarms for toxic and explosive gases, breath alcohol checkers, automatic cooking controls for microwave ovens, air quality/ventilation control systems for homes and automobiles, etc.

Using its innovative gas sensing technologies, Figaro Engineering globally provides cost-effective gas sensing solutions for a wide range of applications in the fields of home and personal safety, industrial safety, air quality control, HVAC, home appliances, and the automotive industry. Figure 1.2 shows the general view of designed system.

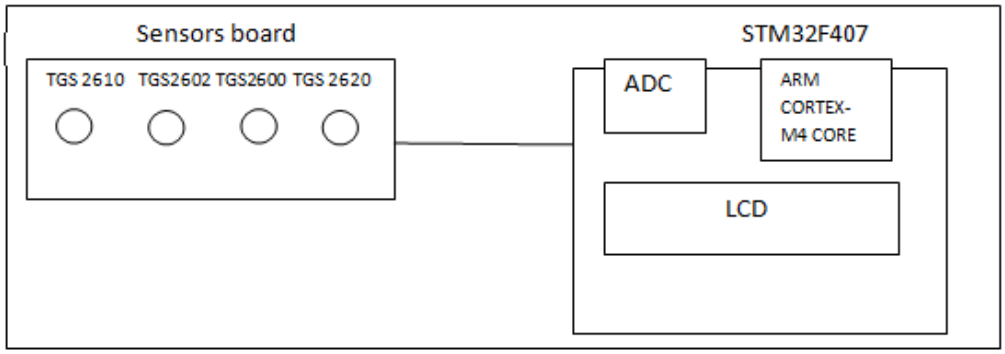

Figure 1.2: General view of designed system

2 REVIEW OF ELECTRONIC OLFACTION

In this chapter, the basics of electronic olfaction and electronic nose technology applied to our work are presented. Through the whole chapter, the relevant aspects of research and development of gas sensors, pattern recognition techniques applied to e-nose data are explained synoptically. Also the materials that appear here have been revised similarly in some related papers concisely [1, 2, 3] and a several textbooks on electronic noses are also available [4].This chapter is presented as a literature review, incorporated with some basic theoretical information.

2.1 Emergence of Artificial Olfaction

As has already been stated the sense of smell is one of the most critical senses in the majority of creatures. It helps in the localization of food sources and the detection of hazards. In addition, in some species smell is considered as a key sense in finding a mate [12]. In humans not only does the sense of smell affect the perceptions of the environment but also the social interactions with others. Nevertheless, in spite of the importance of the olfactory system, humans still lack the appropriate vocabulary to describe odours precisely. Instead, scents are described using ambiguous or abstract terms relating to either personal experience or similarity to other odours [19]. These odour terms not only can vary among individuals but also an individual's perception of odours may change either with a variation in the sensing mechanisms (caused by common cold, aging) or psychological factors. In industrial applications where consumer products are appraised by their olfactory characteristics, the problems of varying a person's realization have developed a need an approach that can be analyzed or quantified in order to be applied in analysis of odours[6]. The field of machine olfaction has emerged as a response to such a requirement. The first efforts to measure the presence of odours commenced as early as the 1920's when Zwaardemaker and Hogewind [20] pondered the electrical charge of a small water sample which constituted a solution of the odorant. Despite the fact that these trials

noted a varied conductivity of different odourous water specimen, no one could develop any real instrumentation. In 1962, Seiyama et al. [21] found that the composition of ambient gases can influence the surface conductance of semiconducting oxides, such as zinc oxide and tin dioxide. Shortly after in 1964, works on an actual experimental tool were published by Hartman et al. [22] who realized that with using a metal wire microelectrode in contact with the surface of a rod saturated with a dilute electrolyte they could measure odours. They also found out that by varying electrodes and electrolyte, a system of several sensors could be used in order to operate at the same time. Later, in 1972, N. Taguchi patented a tin dioxide based chemical gas sensor[13], which later developed into a commercialized product known as the Taguchi Gas Sensor (TGS) [14]. The first published papers and works on odour detection that emphasized dominantly on the problem of data processing and pattern recognition arisen in 1982 in a publication by Persaud et al. [23]. The term "electronic nose" was introduced and later it was redefined by Gardner et al. [24] in order to require two components: a sensing mechanism embracing an array of electronic chemical sensors with modifying selectivity, and an appropriate pattern recognition system. Today, the use of chemical sensors for measuring and analyzing odours is on the increase that attracts interests from the sensor communities and pattern recognition communities. A variety of sensing technology is accessible and currently various kinds of electronic noses benefit from such sensors for numerous commercial applications. To name a few techniques dealing with signal processing we can refer to artificial neural networks (ANN), principal component analytes (PCA) and fuzzy based techniques that have been used with electronic nose data. Since analyzing odours in an efficient and quick way is feasible a number of industrial and research applications such as the monitoring and control of industrial processes, medical diagnosis, and control of food quality have been expanded.

2.2 Electronic Noses

An electronic nose (e-nose) is defined as an instrument that can combine gas sensor arrays and pattern analysis techniques in order to detect, identify the qualification of volatile compounds. As illustrated in Figure 2.1, this process can be divided into three detailed steps: signal preprocessing, dimensionality reduction and prediction.

The initial block in the figure represents the e-nose hardware, which typically includes a gas sensor array, an odor delivery subsystem, an electronic instrumentation stage, and a computer for data acquisition [25].

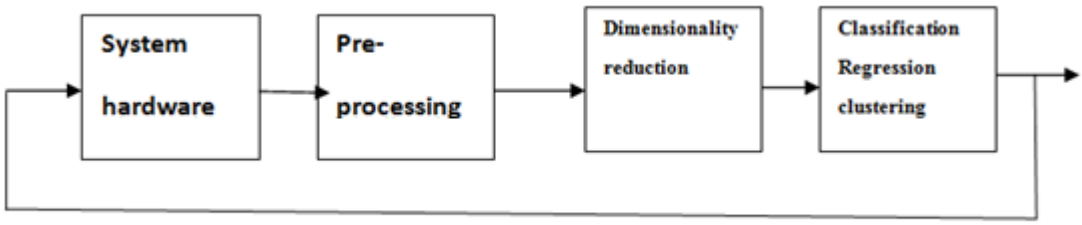

Figure 2.1: Building blocks of the pattern analysis system for an electronic nose.

An electronic nose is typically defined as the following: "An electronic nose is an instrument which is comprised of an array of electronic chemical sensors with partial specificity and an appropriate pattern recognition system which are capable of discerning both simple or complex odours." (Gardner, [26]). The conventional architecture that is used for the identification of odours can be summarized in Figure 2.2. The basic principle originates from the fact that each odour leaves a characteristic pattern or fingerprint of special compounds. Taking into account this hypothesis, the process commences by assembling the signal responses from each sensor, which takes place when the chemical reaction is converted into an electrical signal. The majority of chemical sensors represent a response profile for several analytical methods. The degree of selectivity and the type of odours that are expected to be detected largely depend up on the selection method and the number of sensors. An air tight chamber is used to mount the sensors on that contain gas inlets and outlets to control the gas flow. The signals from each sensor are measured and processed using an analog to digital convertor (A/D) and the whole processor is performed by a computer. After the signal processing, a variety of pre-processing techniques designed to reduce the complexity of the multi-sensor response is applied to transform the data. Afterwards, pattern recognition can be applied to differentiate substances from one another or to train a system in order it o provide a classification based on a collection of known responses[4,6]. The term "electronic nose" is relatively general and hence considering its all capabilities it can be misleading.. Briefly, electronic noses are designed in a way that can mimic the human sense of smell by providing an analysis of individual chemicals or chemical mixtures. They render an efficient way to analyze and compare scents and odours.

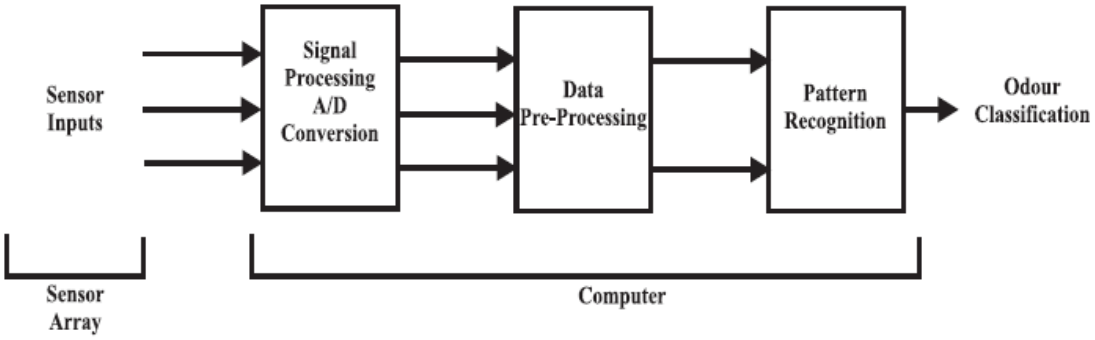

Figure 2.2: An odor classification system [4].

It is essential that electronic noses reach the capability of decomposing odours into their chemical components.

2.3 Sensing Technologies

Several different types of sensing materials are in existence within the field of gas sensors that contribute to the gas sensor. A short list of the commonly used gas sensors include, metal oxide semiconductor [14], conducting polymer sensors [27], acoustic wave sensors [35], field-effect gas sensors [29], pellistors [30], and fiber-optic sensors [31]. Many of these sensing technologies have been discovered empirically and have also been implemented on commercially available electronic noses [32, 33]. Each of these technologies has its own pros and cons over its counterpart and how to select the right kind of gas sensor, depends upon the type of application. Nonetheless, for most the electronic nose applications there are a set of desired properties that tend to be common:

Quick response–On of the abilities of the sensors should be reacting to and recovering from an exposed odour within an acceptable time frame. This is especially of a great importance in applications that integrate electronic nose with a robotic system, such as a mobile robot that should move around an environment and measure odour gradient [34].

Low power consumption–realistically there is a power limitation, and thus the power consumption of the sensors should be relatively low. The headspace containing the sensor array is likely to involve other electrical equipments such as pumps and valves that are mostly supplied with the same power supply.

Compact siz**e**–The smaller the sensor size is ,the easier the integration of sensors in a variety of platforms, including portable electronic noses is .

High sensitivity - Exhibiting a high sensitivity to different odorants and different concentrations of the same odorant by the sensors is mandatory.

Reliability–The behavior of gas sensors particularly over long periods of time ought to be predictable.

Robustness - Unwanted effects arising from humidity and physical motion should not disturb the results from the sensor readings.[6, 28]

In the following subsections a summary of commonly used gas sensing technologies is given. The first type of reaction belongs to reversible process where the analyte ties up to the surface of the sensing material. The inter molecular forces are used to determine the binding between the analyte and the sensing material but binding is usually characterized by a hydrogen bonding. Basically, the analyte does not change but will be separated from the sensing material when the concentration of the odour is removed. This type of reaction has a great similarity to the interaction between odours and receptor proteins in biological systems. A sensor based on this type of reaction, as an example, is the conducting polymer sensors. One of the main advantages of such sensors is that they exhibit both a rapid absorption and de-absorption to gases. The second type of gas sensor, on the other hand, is based on an irreversible reaction. This occurs when an analyte experiences the process of a chemical change at the sensor surface, i.e. catalysis. A very typical sample of this kind of sensor is the Taguchi type SnO2 sensor. High sensitivity to specific odours is believed to be one of the general advantages of the irreversible reaction In these cases, the sensitivity to particular odours is determined by the selection of the catalytic surface. Several kinds of sensing material have been used for the chemical gas sensor. Some examples can be inorganic crystalline or pollycrtalline, organic materials and polymers and it is fairly rare but even biologically materials such as proteins and enzymes have been used. In the following subsections, more common types of sensors will be discussed is given.

2.3.1 Metal oxide semiconductor field-effect transistor (MOSFET) sensors

The general structure of the metal oxide semiconductor field effect transistor (MOSFET) is shown in Figure 2.3. The sensor is consisting of three components: a

catalytic metal, an insulator and a transistor (semiconductor). The basic principle of the device allows gaseous compounds to react with the catalytic metal and produce types that are able to be diffused through the metal film and be absorbed onto a metal insulator. A voltage change δV will occur due to the absorption, and hence the current-voltage characteristics of the sensor will change. Different catalytic metals might be used in order to vary the sensitivities of the sensor, For instance, while using palladium high sensitivity to hydrogen is displayed by the sensing characteristics [4, 6, and 28]. The MOSFET operates in an area whose temperature varies between 50 ◦C to 150 ◦C in order to enhance the rate of catalytic reactions on the metal surface and to prevent the absorption of water molecules. In the case of the hydrogen sensor, the typical response time is approximately 5 seconds for 50 PPM hydrogen in the air. The sensitivity of the catalytic metal can be reduced by some physical effects [28].

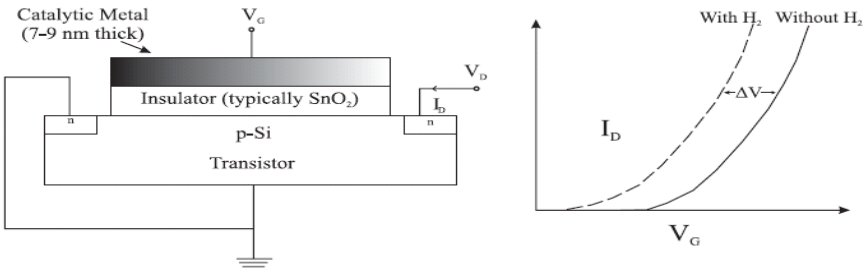

Figure 2.3: MOSFET structure and the current-voltage characteristics The gate voltage is denoted by VG and drain current ID[28].

2.3.2 Semiconducting metal oxide sensors (MOS)

Gas sensing technology, which is based on the chemical sensitivity of semiconducting metal oxides, has been widely used to make arrays for the measurement of odor rather than any other classes of gas sensors. In much of the early research on electronic noses, the MOS has been the most domineering technology for constructing the sensor arrays. The MOS is analogous to the MOSFET in terms of operating principle and is composed of a heating element coated with a semiconductor, most typically tin dioxide (SnO2). The sensing material is then doped with small amounts of catalytic metal additives for e.g. palladium or platinum. The doping of the sensor causes the operating conditions to be changed by changing the particle size of the sintered material; accordingly an effect will be shown up on the selectivity of the sensor to different substances. The Figaro

Engineering Company has been one of the major manufacturers of the MOS sensor whose sensors were developed by N. Taguchi [14]. Some examples of different types of the Taguchi Gas Sensor (TGS) and their odour sensitivities are given in Table 2.1.

Table 2.1: Examples of commercially available SnO2 sensors provided by the Figaro Engineering Company [6, 28].

Sensor Model	Category of Odours Detected
TGS 800	Air Contaminants
TGS 813	Combustible Gas
TGS 826	Toxic Gases (Ammonia)
TGS 825	Toxic Gases (Hydrogen Sulfide)
TGS 880	Cooking Vapours

The main functionality of TGS sensors is by allowing electrical current to flow through the grain boundaries of the SnO2 micro-crystal surface. At the grain boundary, oxygen is absorbed and as a result potential barrier is formed. The size of this potential barrier is reflected in the value of the sensor's resistance, the higher the barriers, the more resistance across the sensor is (see Figure 2.4)[6,28]. On the contrary, exposure to a deoxidizing gas will deplete the grain boundaries and thus electrical charge flows more freely and the overall resistance is reduced.

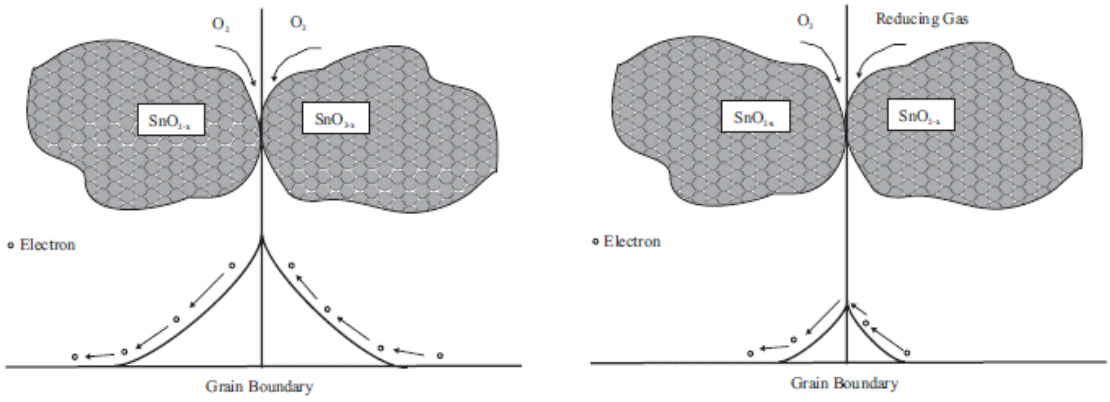

Figure 2.4: Model of the inter-grain potential barrier in the absence of a gas (left) and the presence of gases (right)[6].

The following equation expresses the relationship between the concentration of deoxidizing gas and the sensor resistance.

$$R = AC^{-\alpha} \quad \textbf{(2.1)}$$

Where R is the resistance of the sensor, A and α are both constants and C represents the concentration of the sampling gas. Typically the relationship between the sensor resistance and the concentration of deoxidising gas is linear on a logarithmic scale within a range of concentration (up to several thousand PPM). Normally each sensor is sensitive to several deoxidising gases, with the highest sensitivity to an optimized gas which is determined by the fabrication of the physical sensing materials. The sensor's behavior with relation to the varying concentration of gas is shown graphically in Figure2.5. Supplying an input power source for the internal heater can be the final requirement of sensor operation. If the sensors are heated to a high temperature, between 300◦C and 500◦C the sensitivity characteristics will increase. This is partly due to the fact that the rate of reactions on the oxide surface increases provided that the temperature exceeds 200◦C. Additionally, to avoid covering the sensor surface with water particles, the temperature of the sensor should remain above 100◦C. One of the advantages of the MOS sensor is because of its high sensitivity to specific gases in the order of 10−500 PPM.

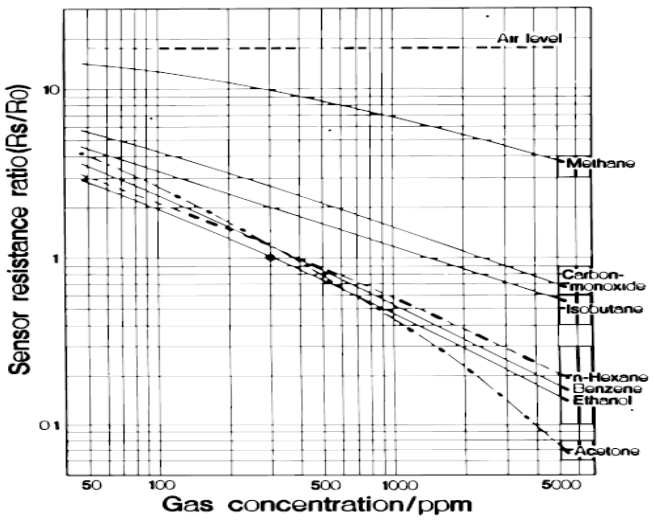

Figure 2.5: Sensitivity characteristics of the TGS822 sensor to ethanol vapour and other various gases and vapours. The ordinate is the ratio of the sensor's resistances measured at various concentrations of gases compared to the sensor resistance at 300 PPM ethanol vapour, provided by [14].

Perhaps the most attractive feature of these gas sensors is their low effectiveness and the usability of the life span of 3−5 years, depending on the usage of the sensor.

A few drawbacks of the sensors however, can be attributed to the inter dependency between external humidity and temperature effects to the rate of reaction to a gas, and high power consumption [4, 6, 28].

2.3.3 Conducting polymer sensors

Another popular sensing technology based on measuring the resistance of a thin film polymer (electropolymerization) is called conducting polymers that are an example of reversible reaction gas sensing type. Typical polymers are constructed from monomers such as pyrrole, aniline or thiophene. Conducting polymers differ from the metal oxide sensor since, they are sensitive to a wide variety of organic vapours. In addition, the devices are small with low power consumption and can operate at room temperature. In this thesis the conducting polymer sensors are mostly used in experimental validations[6, 28].

2.3.4 Acoustic sensors

Electroacoustic devices based on the piezoelectrical properties of quartz material have

been successfully used for implementation of sensors since 1964 (King 1964). These sensors are based on the propagation of acoustic waves produced by piezoelectrical materials (e.g. quartz or LiNbO3 or Si-SiO2-ZnO) in a multi-layer structure (Lucklum and Hauptmann 2000).The most common of those acoustic sensors are Surface acoustic wave (SAW) and bulk acoustic wave (BAW). The operation mode of these sensors is determined by the physical changes produced on their membranes made of chemically interactive materials (CIM). When a gas specific sensing film is placed on the surface of the device, the application of the SAW or BAW device can be achieved. The exposure of the sensing film to the target gas, mechanical and electrical perturbations in the sensing film will cause a corresponding change in the oscillation frequency of the acoustic wave device oscillator [28, 36].

2.3.5 Biosensors

A biosensor consisting of an immobilised biologic molecule (enzymes, cellules or antibodies) next to a transducer can transform a chemical signal into an electric signal or into other kind of output as optical, acoustic and heat signal when an analyte reaches to it. Biosensors can also be defined as “a selfcontained analytical

device that responds selectively and reversibly to the concentration or activity of chemical species in biological samples". Based on the characteristics of biological elements , the biosensors can be clustered into three great main groups: metabolism biosensors (enzymes, combinations of enzymes and cofactors, and cells like algae and bacteria), affinity biosensors (antibodies, "immunosensors") and recombinant biosensors (DNA probes). The transduction element allows the chemical signals which are obtained from a biological process to be transformed into another kind of signal. Biosensors can also be stratified into electrochemical (amperometric, potentiometric, conductimetric), optical, calorimetric and acoustic biosensors (Griffiths and Hall 1993) [28].

2.4 Data Processing Techniques

2.4.1 Pre-processing

After an odor has been sampled by the array and the information is stored in the PC, the analysis of the data will begin .The data is mostly multi-dimensional and the objectives of the data pre-processing are the following [4, 6]. It might be useful to reduce the noise and anomalous data readings that are traced back to both the sampling frequency and the analogue to digital conversion. The range of the sensor data can be fixed by normalisation of the sensor data or re-scaling techniques, typically between 0 and 1. There are two motivations behind data normalization. The first one is to cope with multi sensor inputs that may be of varying magnitudes. The second, the processing time for many pattern recognition techniques such as an ANN can be decreased when the whole input variables are of the same magnitude. Compensation for the reference gas before the application of pattern recognition techniques can be beneficial .For Compensation the variations in the initial or steady state values are considered that may be te result of drift or change in environmental conditions. The main purpose of data reduction is to understand the relationship between each of the sensor's response and the odor . Typically, it is attempted to reduce the complexity or dimensionality of the data by eliminating the co-dependencies. Many statistical techniques are available for this process and some of

the them can also be applied to perform pattern recognition, such as principal component analysis that will be mentioned in the next section [6].

2.4.2 Pattern analysis for machine olfaction

The major problem with data analysis from an electronic nose is determining the relationship that exists between a set of independent variables (the output from n sensors) and a set of dependent variables (odour classes) [37]. The processing of electronic nose data can be divided into two different approaches while applying to multivariate analysis. The first approach is a statistical one. The second approach is a biologically inspired one using a manner similar to human cognitive processing, namely a neural network. The classification tree by [37] shown in Figure 2.6 is an illustration of the subdivision of the various pattern recognition techniques. Pattern analysis includes a critical building block in the development of gas sensor array instruments which is capable of detecting, identifying, and measuring volatile compounds; a technology that has been proposed as an artificial substitute of the human olfactory system. In order to design a pattern analysis system that can work successfully for machine olfaction, it is required that a the various issues involved in processing multivariate data such as signal-preprocessing, feature extraction, feature selection, classification, regression, clustering, and validation be considered meticulously. There is quite a few methods from statistical pattern recognition including neural networks, machine learning, and biological cybernetics that have been employed in the process of electronic nose data.[4] In this section , comprehensive set of pattern recognition(PARC) techniques employed to analyze electronic nose (EN) data are being described in more details ; The methods that are being described here are mostly common conventional statistical methods, such as principal components analysis (PCA).Then the development of biologically motivated non-parametric methodologies, such as artificial neural networks (ANNS) including multi-layer perceptron (MLP), and K-nearest neighbor(KNN) analysis methods are briefly explored . It is appreciable to note that PCA methods can be used to extract features in order to reduce the dimension of data while the other two methods are generally used as classifiers.

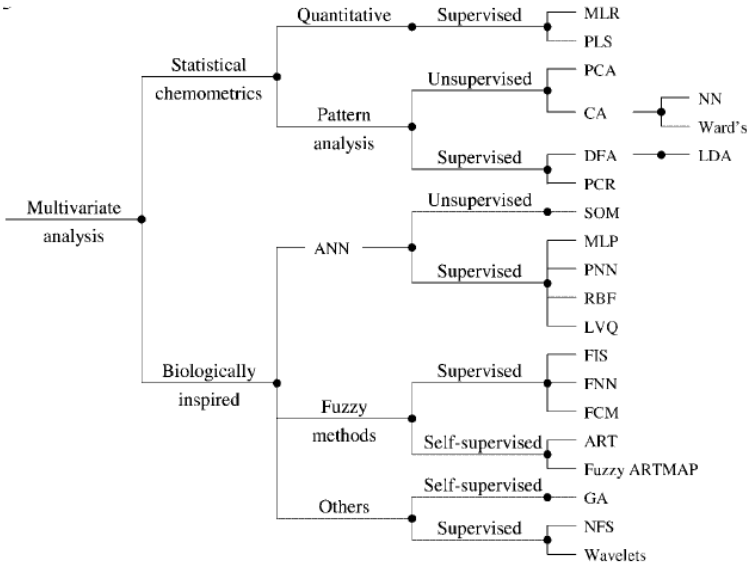

Figure 2.6: Classification scheme presented by [48] of the multivariate data processing techniques commonly employed to analyze data from electronic nose instrumentation [37].

2.4.2.1 Principal component analysis (PCA)

PCA is responsible for the performance of a principal component or eigenvector analysis of the data and projection of the samples into a new co-ordinate system. The most applicable feature of PCA is its capability of describing major trends in the data by reducing the dimensionality of the data. In other words, the systematic variations existing in the original data set can be described with the help of fewer variables. As a result, PCA can be used as a pre-processing technique. The principal components are often used as inputs or features into further processing algorithms assuming non-linear type classification [38]. More specifically, the dataset is transformed into a new coordinate system by PCA in a way that the projection onto the first coordinate has the greatest variance among all possible projections, and the projection onto the second coordinate has the second greatest variance, and so on. Finding these successive coordinates (or principal components) provides us with the ability to visualize the distribution of the original dataset after projecting it onto a low-dimensional space. In other words, PCA is capable of providing the best meaningful observable angle that can disperse the dataset as much as possible. Here, set of instruction pertaining to the mathematics underlying PCA are reviewed as follows.[39, 40]

The step by step guide for performing PCA on a dataset is as fallowing:

1. First the sample mean of dataset is calculated:

$$\mu = \frac{1}{n}\sum_{i=1}^{n} x_i \quad \textbf{(2.2)}$$

2. Then ,compute the covariance matrix

$$C = \frac{1}{n}\sum_{i=1}^{n}(x_i - \mu)(x_i - \mu)^T \quad \textbf{(2.3)}$$

3. Next, the eigen values of c are computed and arranged afterwards in a descending order $\{ \lambda_1, \lambda_2, \dots, \lambda_d \}$, with the corresponding eigenvectors $\{U_1, U_2, \dots, U_d\}$.
4. The transformation matrix is then U^T , with $U = [U_1, U_2, \dots, U_d]$. Namely, vector X after transformation is $y = U^T.x$. If the purpose is to keep the first 3 dimensions, simply put the first 3 Eigenvectors (U_1, U_2, U_3) are put into U directly.

2.4.2.2 Multilayer perceptron neural network (MLP)

In a network, the elements, which are being processed, are organized in a regular architecture of three distinct groups of neurons: input, hidden, and output layers. The only units including neurons can be found in the hidden and output and so an MLP has two layers of weights. The number of input nodes is typically determined to correspond to the number of sensors in the array. The number of neurones in the hidden layer is determined experimentally and generally the number of odors analyzed determines the number of output neurones. When using a one-in-N coding scheme, one output neuron for each potential odor classis specified. There are more efficient coding schemes but the abovementioned one is the simplest. An MLP has a supervised learning phase, which employs a set of training vectors, followed by the prediction, test or recall phase of unknown input vectors. The topology of a network used to identify five alcoholic odors using a twelve-element tin-oxide sensor EN is depicted in Figure 2.7. MLP, whose learning algorithm is BP, has been applied to the prediction of bacteria type and culture growth phase using an array of six different metal-oxide semiconductor gas sensors. As the results show the best MLP was able to classify 96% of unknown samples on the basis of 360 training vectors and 360 test vectors very successfully. While BP is being used to train the network, it is necessary to provide it with a number of sample inputs (training set) with corresponding target outputs.

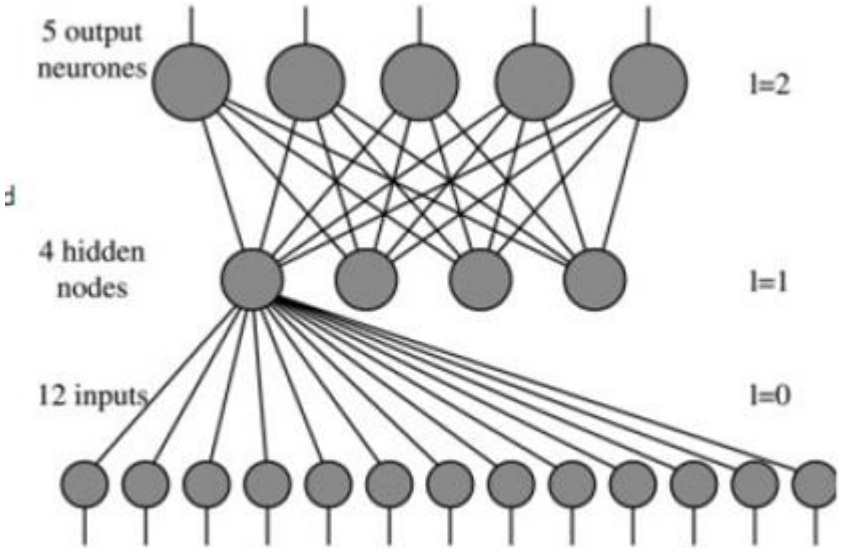

Figure 2.7: Structure of fully connected 3 layer back propagation network used to process data From 12-element in oxide EN for five alcoholic odors [4].

Each neuron computes its weighted inputs and performs a non-linear transformation of this sum using a presumed activation function, for example a sigmoid transfer function that constrains the output to a value between [0,1] or [_1,1] [4]. For more clarification, of the subject, the algorithm is being explained in more details as follows. Neural networks (NN) can be used to solve non -linear and complex functions. When it is used to design Multi-Input Single-Output (MISO) systems, NN map n-dimension inputs to single dimension output. In this study, A NN has the functionality of pattern recognition of electronic nose to identify certain gas. The Neurons in artificial intelligence act as a biological nerve. Several inputs (x) are multiplied to each appropriate weight (w) [43].

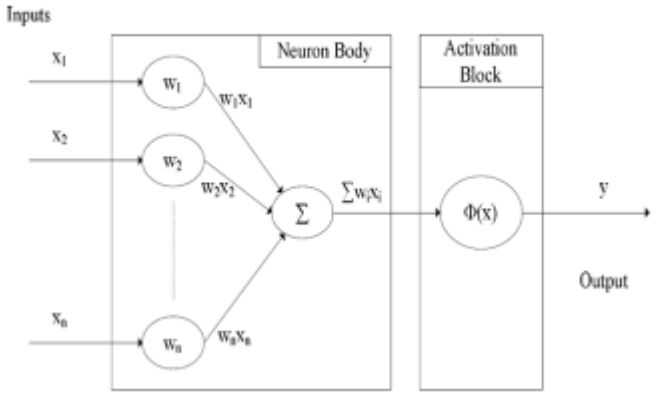

Figure 2.8: Neuron Model [43]

Then the total result of multiplication with the output from inside activation function is added to take a single-degree output F(x, w), this process can be seen in Figure 2.8

$$in_i = \sum_j w_{ji} * a_j \quad \textbf{(2.11)}$$

To activate each neuron in a neural network an activation function is required such as hyperbolic function, step, impulse and sigmoid. Sigmoid function as shown in Figure 2.9, is closer to the real function of brain when compared to other activation function , so it's often used in many research. A set of neurons can turn to a network which can act as a computation equipment to solve problem. The solution differs from architecture to another based on the number of neurons in network. A general architecture of neural networks can be seen in Figure 2.10.

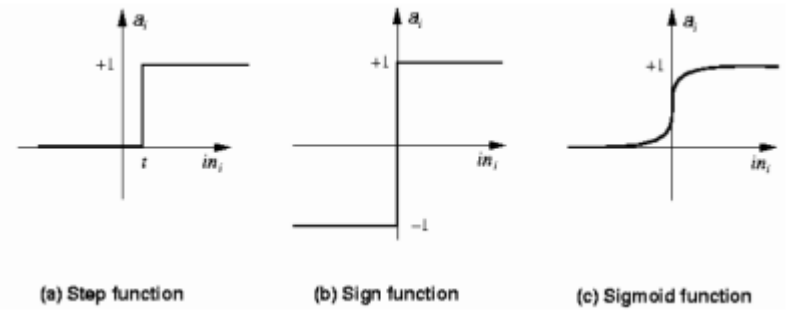

Figure 2.9: Activation Function

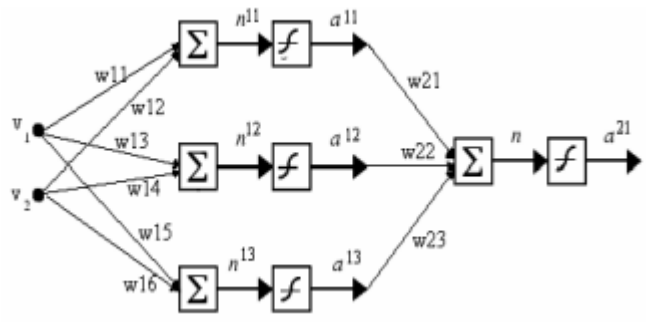

Figure 2.10: Architecture Neural Network [43]

2.4.2.3 Nearest neighbor classifier (KNN)

K-nearest neighbor algorithm (KNN) is a part of supervised learning that has been widely used in many applications in the field of data mining, statistical pattern recognition and so forth. KNN is a method for classification of objects based on the

closest training examples in the feature space. An object is classified by the vote of majority of its neighbors. K is always a positive integer. The neighbors are taken from a set of objects for which the correct classification is known. Among other distance measures such as the Manhattean distance, the Euclidean distance is more frequently used .

Distance Functions

Euclidean	$\sqrt{\sum(x_i - y_i)^2}$
Manhatan	$\sum\|x_i - y_i\|$
Minkowski	$(\sum(\|x_i - y_i\|)^q)^{1/q}$

The algorithm on how to compute the K-nearest neighbors is as follows:

1. First, the parameter K = number of nearest neighbors beforehand is determined. Based on the requirements K can take different values.
2. Second, the distance between the query-instance and all the training samples is calculated. Any distance algorithm can be optionally applied.
3. Then, the distances for all the training samples are sorted and the nearest neighbor is determined based on the K-th minimum distance.
4. Next, Since this is supervised learning, all the Categories of the training data for the sorted value which fall under K are being taken
5. Finally, the majority of nearest neighbors are used as the prediction value.

3 STM32F407, A CORTEX-M4 BASED EMBEDDED SYSTEM

In this chapter some general information regarding Microcontroller, Discovery board and programming software Environment will be explained. Then general contents and features of each part will be discussed.

3.1 Microcontroller

Microcontrollers are often described as single chip computers. They contain a microprocessor core, (often) some memory and various “peripheral” devices such as parallel i/o ports, serial i/o ports, timers, analogue to digital converters (ADC's) and various other special function sub-systems.

3.1 .1 STM32F Overview

ST is introducing STM32 products based on Cortex M4 core. Over 30 new part numbers pin-to-pin and software that are compatible with the existing STM32 F4 Series. The new DSP and FPU instructions that have been combined to 168 Mhz performance have opened agate way to a new level of Digital Signal Controller applications and faster development time. Figure 3.1 illustrates STM 32 F4 block diagram [52, 53]. Among different options of Cortex™-M4 microcontroller family, STM32F407xx series was chosen here to be applied in the project. Cortex™-M4 32-bit RISC core operates frequencies up to 168 MHz. The Cortex-M4core features a floating point unit (FPU) single precision which supports all ARM single precision data-processing instructions and data types. It also implements a full set of DSP instructions and a memory protection unit (MPU) for the sake of enhancement of security. The Cortex-M4 core with FPU will be referred to as Cortex-M4F throughout this document. The STM32F407xx family incorporates high-speed embedded memories (Flash memory up to 1 Mbyte, up to 192 Kbytes of SRAM), up to 4 Kbytes of backup SRAM, and an extensive range of enhanced I/Os and

peripherals connected to two APB buses, three AHB buses and a 32-bit multi-AHB bus matrix.

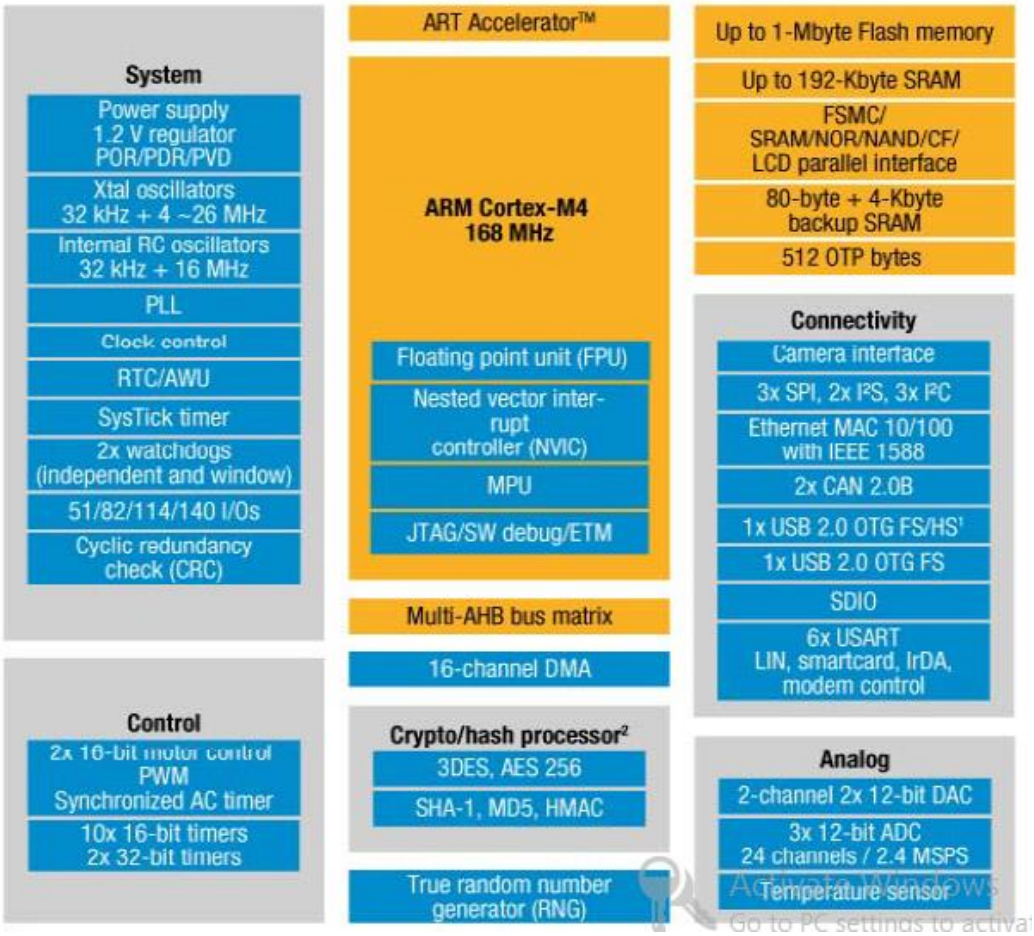

Figure 3.1: STM 32 F4 block diagram[57].

All devices proffer three 12-bit ADCs, two DACs, a low-power RTC, twelve general-purpose16-bit timers including two PWM timers for motor control, two general-purpose 32-bit timers and a true random number generator (RNG). In addition, standard and advanced communication interfaces can be featured.

● Up to three I2Cs

● Three SPIs, two I2Ss full duplex. To achieve audio class accuracy, the I2S peripherals

can be clocked via a dedicated internal audio PLL or via an external clock to allow synchronization.

● Four USARTs plus two UARTs

● An USB OTG full-speed and a USB OTG high-speed with full-speed capability (with the ULPI),

● Two CANs

● An SDIO/MMC interface

● Ethernet and the camera interface available only on STM32F407xx devices only.

New advanced peripherals include an SDIO, an enhanced flexible static memory control

(FSMC) interface (for devices offered in packages of 100 pins and more), a camera interface for CMOS sensors.

The STM32F407xx family operates in the temperatures ranging from –40 to +105 °C and a power supply working in the range of 1.8 to 3.6 V. There will be a drop in the voltage of supply voltage up to 1.7 V so long as the operating temperature varies between 0 to 70 °C and an inverted reset signal is applied to PDR_ON. Low power applications are attainable with the aid of a comprehensive set of power-saving mode. The STM32F407xx family offers devices in various packages ranging from 64 pins to 176 pins. The set of included peripherals is modified in accordance with the selected device. These features make the d STM32F407xx microcontroller family very appropriate for a wide range of applications as follows

● Motor drive and control applications

● Medical equipments

● Industrial applications: PLC, inverters, circuit breakers

● Printers, and scanners

● Alarm systems, video intercom, and HVAC and Home audio appliances[52, 53, 54].

3.1.2 Components of STM32F407 MCU

This main concern of this section is to explain the microcontroller core, memories, I/Os and peripherals introduced at the block figure 3.2. There are brief explanations of parts and peripherals of STM32F407 microcontroller as below

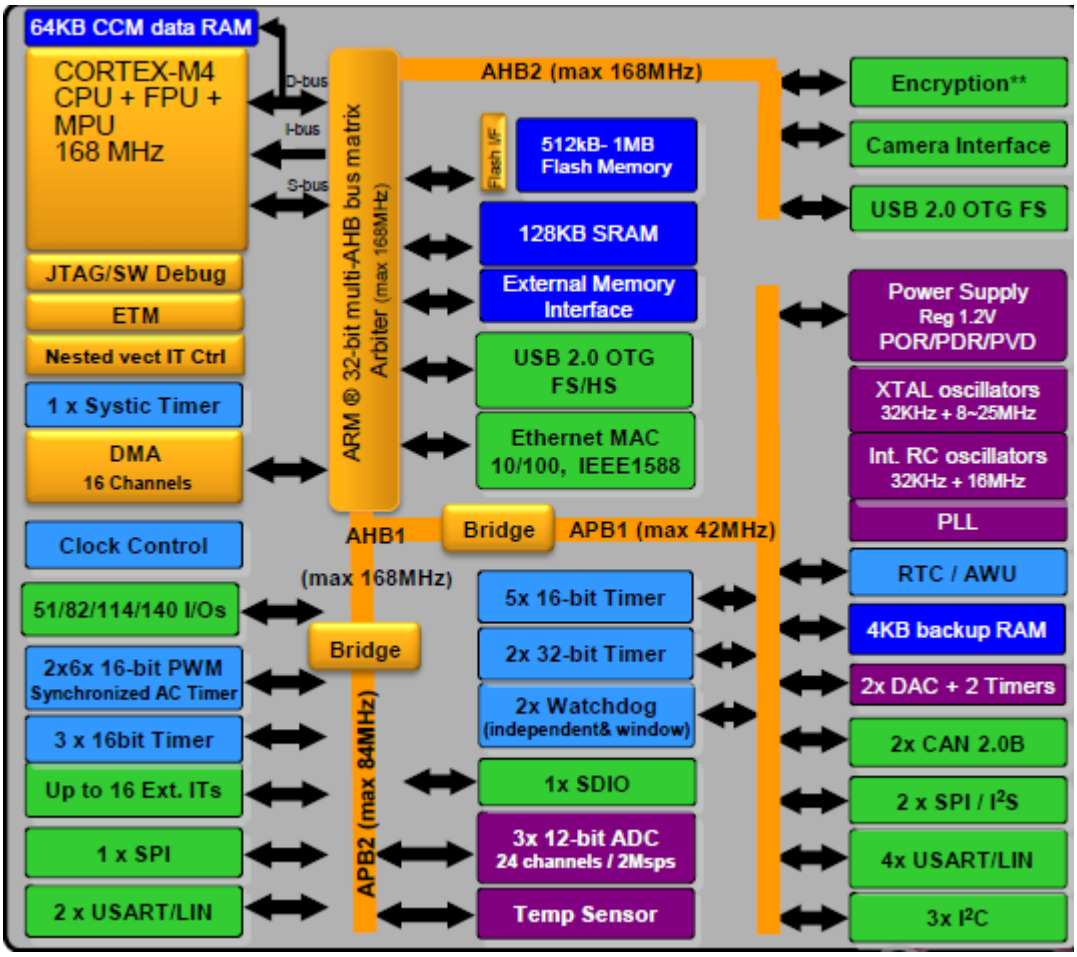

Figure 3.2: STM32F4xx Block Diagram [57].

3.1.3 ARM Cortex-M4 core with embedded Flash and SRAM

The ARM Cortex-M4F processor is the latest generation of ARM processors for embedded Systems. The main purpose for developing this processor is to provide an inexpensive platform that meets the requirements of MCU implementation, with a reduced pin count and low-power consumption whereas delivering an outstanding computational performance and an advanced response to interrupts. The ARM Cortex-M4F 32-bit RISC processor features exceptional code-efficiency delivering the high-performance which is expected from an ARM core in the memory size dealing with 8- and 16-bit devices. The processor supports a set of DSP instructions which allow efficient signal processing and complex algorithm execution. Its single precision FPU (floating point unit) accelerates the software development by using Meta language development tools, while avoiding saturation. The STM32F407xx family is matchable with all ARM tools and softwares. In this thesis, inasmuch as

processing algorithms are implemented, DSP and FPU parts are of a great importance [52, 53, 54].

3.1.4 Memory protection unit

The management of accessibility of CPU in order to prevent one task from fortuitous corruption of memory or resources used by any other active task is done by the memory protection unit (MPU). This memory area is well organized into up to 8 protected areas that can in turn be subdivided up into 8 areas. The sizes of protection area are between 32 bytes and the whole 4 gigabytes of addressable memory. The MPU is especially helpful for applications in which some critical or certified codes have to be protected against the misbehavior of other tasks. The RTOS (real time operating system) is responsible to manage this malfunction [52, 53, 54].

3.1.5 Embedded flash memory

A flash memory of 512 Kbytes or 1 Mbytes, which is available for storing programs and data ,is embedded by the STM32F40x devices [52].

3.1.6 CRC (cyclic redundancy check) calculation unit

The CRC (cyclic redundancy check) calculation unit is used to get a CRC code from a 32-bitdata word and a fixed generator polynomial. Among other applications, CRC-based techniques are used to corroborate data transmission or storage integrity. In the scope of the EN/IEC 60335-1 standard, they offer a means of upholding the flash memory integrity. The CRC calculation unit can help compute a software signature during runtime, to be measured and compared with a reference signature that has been generated at link-time and then stored at a given memory location [52, 53, 54].

3.1.7 Embedded SRAM

All STM32F40x products are able to embed:

● Up to 192 Kbytes of system SRAM including 64 Kbytes of CCM (core coupled memory) data RAM .RAM memory is accessed (read/write) at CPU clock speed with 0 wait states.

● 4 Kbytes of backup SRAM

This area is accessible only for the CPU. Its content is protected against possible undesirable write accesses, and is kept in Standby or VBAT mode [52, 53, 54].

3.1.8 Multi-AHB bus matrix

The 32-bit multi-AHB bus matrix interlinks all the masters (CPU, DMAs, Ethernet, USBHS) and the slaves (Flash memory, RAM, FSMC, AHB and APB peripherals) and ensures an efficient operation even on circumstances that several high-speed peripherals work simultaneously [52, 53, 54].

3.1.9 Direct Memory Access (DMA)

Two general-purpose dual-port DMAs (DMA1 and DMA2) with 8streams each are featured by the STM32F40x devices. They are able to manage memory-to-memory, peripheral-to-memory and memory-to-peripheral transfers. They are designed to provide the maximum peripheral bandwidth (AHB/APB) and dedicated FIFOs for APB/AHB peripherals, support burst transfer can be featured by them as well. The two DMA controllers support circular buffer management, so there is no need to any specific code when the controller reaches the end of the buffer. The two DMA controllers also have a double buffering feature for automation of the use and switching of two memory buffers without requiring any special code. Each stream is connected to dedicated hardware DMA requests having a support for the software trigger on each stream. The configuration is made by the software and transfer sizes between source and destination are independent. The DMA can be used with the main peripherals [52, 53, 54]:

- SPI and I2S
- I2C
- USART
- General-purpose, basic and advanced-control timers TIMx
- DAC
- SDIO
- Camera interface (DCMI)
- ADC

3.1.10 LCD parallel interface

The FSMC can be configured to interface seamlessly with most graphic LCD controllers. The Intel 8080 and Motorola 6800 modes can be supported by the ESMC which is flexible enough to be adapted to specific LCD interfaces. The parallel interface capability of this LCD simplifies building cost effective graphic applications using LCD modules with embedded controllers or high performance solutions using external controllers with dedicated acceleration[52, 53, 54].

3.1.11 Clocks and startup

As a default CPU clock the 16 MHz internal RC oscillator is selected on reset. The 16 MHz internal RC oscillator is factory-trimmed to offer 1% accuracy over the full temperature range. Then application is authorized to choose either the RC oscillator or an external 4-26 MHz clock source as system clock. This clock can be monitored to detect failure. In the case of a failure being detected, the system automatically switches back to the internal RC oscillator and a software interrupt is generated (if enabled). This clock source acts as the input to a PLL thus allowing to increase the frequency up to 168MHz. Similarly, full interrupt management of the PLL clock entry is accessible if necessary (for example if an indirectly used external oscillator fails). The configuration of the three AHB buses, the high-speed APB (APB2) and the low-speed APB (APB1) domains can be allowed by several prescalers. The maximum frequency of the three AHB buses is 168 MHz whereas the maximum frequency of the high-speed APB domains is 84MHz. The maximum permissible frequency of the low-speed APB domain is 42MHz. The devices embed an allocated PLL (PLLI2S) which allows to achieve audio class performance. In this case, the I2S master clock can generate all standard sampling frequencies from 8 kHz to 192 kHz [52, 53, 54].

3.1.12 General-purpose input/outputs (GPIOs)

Each pin of the GPIO can be configured by software as output (push-pull or open-drain, with or without pull-up or pull-down), as input (floating, with or without pull-up or pull-down) or as peripheral alternate function. Digital or analog alternate functions share the majority of the GPIO pins. All GPIOs are high-current-capable and have the capability of speed selection to manage internal noise in, power

consumption and electromagnetic emission a better way. If mandatory, the I/O configuration can be locked following a specific sequence in order to avoid spurious writing to the I/Os registers. Fast I/O handling allows the maximum I/O toggling up to 84 MHz [52, 53, 54].

3.1.13 Analog-to-digital converters (ADCs)

There are three 12-bit analog-to-digital converters which are embedded and each of them shares up to 16external channels that can perform conversions in the single-shot or scan mode. In the scan mode, conversion is automatically performed on a selected group of analog inputs.

Extra logic functions that are embedded in the ADC interface allow:

- Simultaneous sample and hold
- Interleaved sample and hold

The DMA controller can act as a server to the ADC. An analog watchdog feature allows to monitor converted voltage of one or more selected channels very precisely. An interruption can be created provided that the converted voltage is outside the programmed thresholds. For synchronization of A/D conversion and timers, the ADCs could be triggered by any of TIM1, TIM2, TIM3, TIM4, TIM5, or TIM8 timers [52, 53, 54].

3.2 STM32F4 DISCOVERY

The STM32F4 high-performance features can be found with the help of the STM32F4DISCOVERY. It works upon the basis of an STM32F407VGT6 and consists of an ST-LINK/V2 that has embedded debug tool interface, ST MEMS digital accelerometer, ST MEMS digital microphone, audio DAC with integrated class D speaker driver, LEDs, push button sand a USB OTG micro-AB connector[55, 56].

Figure 3.3: STM32F4DISCOVERY board[55].

3.2.1 Features

Hereafter, in this section general features and capabilities of discovery board will be mentioned. The STM32F4DISCOVERY exhibits the following features:

● STM32F407VGT6 microcontroller featuring 1 MB of Flash memory, 192 KB of RAM in an LQFP100 package

● On-board ST-LINK/V2 with selection mode switch to use the kit as a standalone

ST-LINK/V2 (with SWD connector for programming and debugging)

● Board power supply: through USB bus or from an external 5V supply voltage

● External application power supply: 3V and 5V

● LIS302DL, ST MEMS motion sensor, 3-axis digital output accelerometer

● MP45DT02, ST MEMS audio sensor, omnidirectional digital microphone

● CS43L22, audio DAC with integrated class D speaker driver

● Eight LEDs:

– LD1 (red/green) for USB communication

– LD2 (red) for 3.3V power on

– Four user LEDs, LD3 (orange), LD4 (green), LD5 (red) and LD6 (blue)

– 2 USB OTG LEDs LD7 (green) VBus and LD8 (red) over-current

● Two pushbuttons (user and reset)

● USB OTG with micro-AB connector

● Extension header for LQFP100 I/Os for quick connection to prototyping board and easy Probing[55, 56].

3.2.2. Hardware and layout

The STM32F4DISCOVERY is designed adjacent to the STM32F407VGT6 microcontroller in a100-pin LQFP package. The interconnections and links between the STM32F407VGT6 and its peripherals (STLINK/ V2, pushbutton, LED, Audio DAC, USB, ST MEMS accelerometer, ST MEMS microphone, and connectors) are illustrated in Figure 3.4[55, 56].

3.2.3. STM32F407VGT6 microcontroller

This ARM Cortex-M4 32-bit MCU with FPU has 210 DMIPS, up to 1 MB Flash/192+4 KBRAM, USB OTG HS/FS, Ethernet, 17 TIMs, 3 ADCs, 15 comm. interfaces and a camera. Features and peripherals of microcontroller were mentioned earlier mentioned in section3.1.

3.2.4. Power supply

The power supply can be provided either by the host PC through the USB cable, or by an external5V power supply. The main duty of diodes D1 and D2 is protecting the 5V and 3V pins from external power supplies:

● 5V and 3V can be used as output power supplies in the case that another application board is connected to pins P1 and P2. Under this circumstance, the 5V and 3V pins

deliver a 5V or 3V power supply and it is required that power consumption be lower than 100 mA.

● Applying 5V as input power supplies is also feasible e.g. when the USB connector is not connected to the PC. In this case, the power of STM32F4DISCOVERY board must be supplied by a power supply unit or by auxiliary equipment which is conformable with standard EN-60950-1: 2006+A11/2009, and must be Safety Extra Low Voltage (SELV) with limited power capability[55, 56].

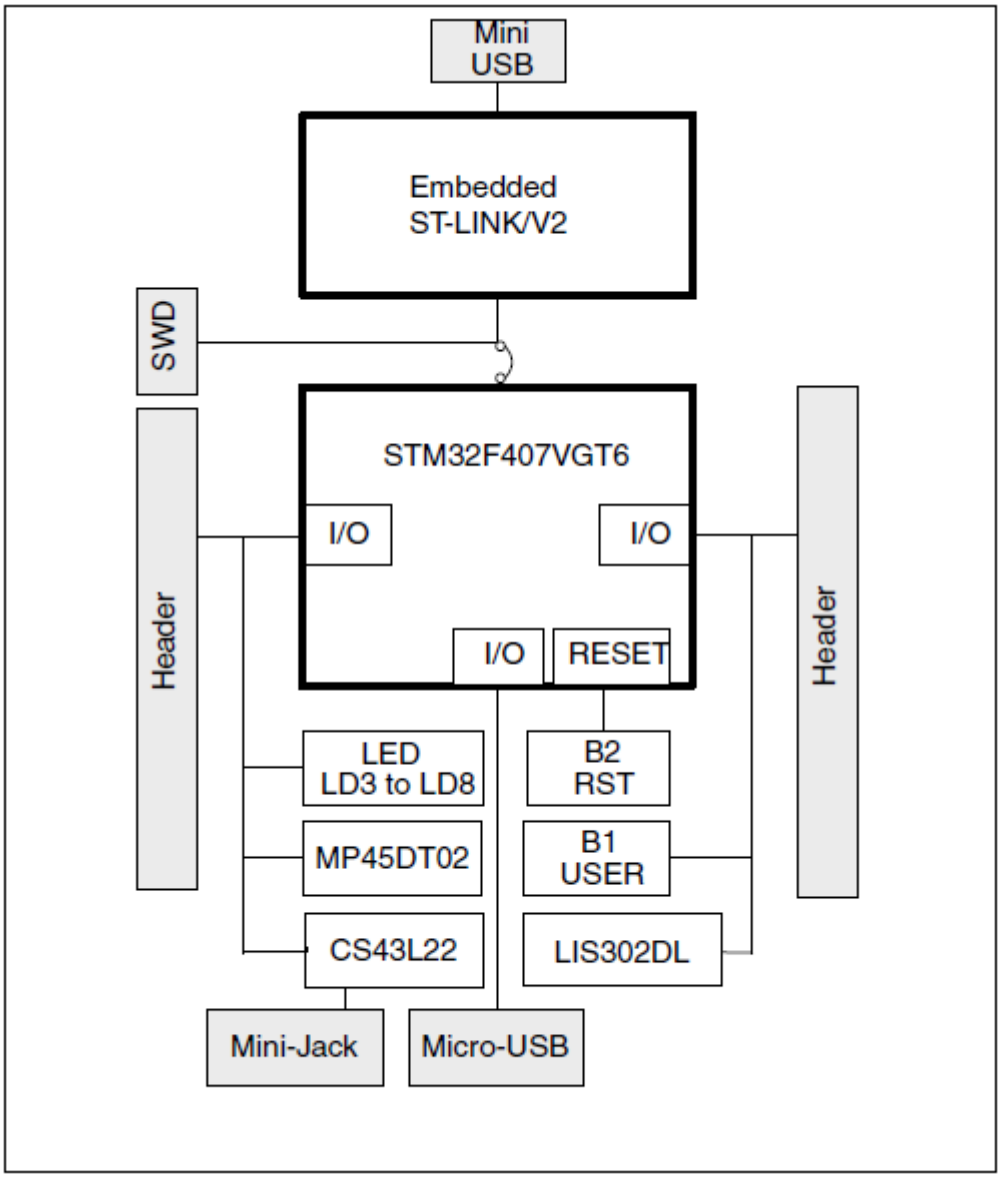

Figure 3.4 Hardware block diagram [56].

3.3 MDK-ARM Microcontroller Development Kit

In this section important part of Keil MDK-ARM™ (Microcontroller Development Kit) will be explained. Figure 3.5 Shows MDK version5 developer environment.

3.3.1 What is MDK?

Keil MDK-ARM™ (Microcontroller Development Kit) is a complete software development environment for ARM processor-based microcontrollers . MDK helps

to create embedded applications for ARM Cortex-M processor-based devices. MDK version 5 split into the MDK Core and Software Packs.

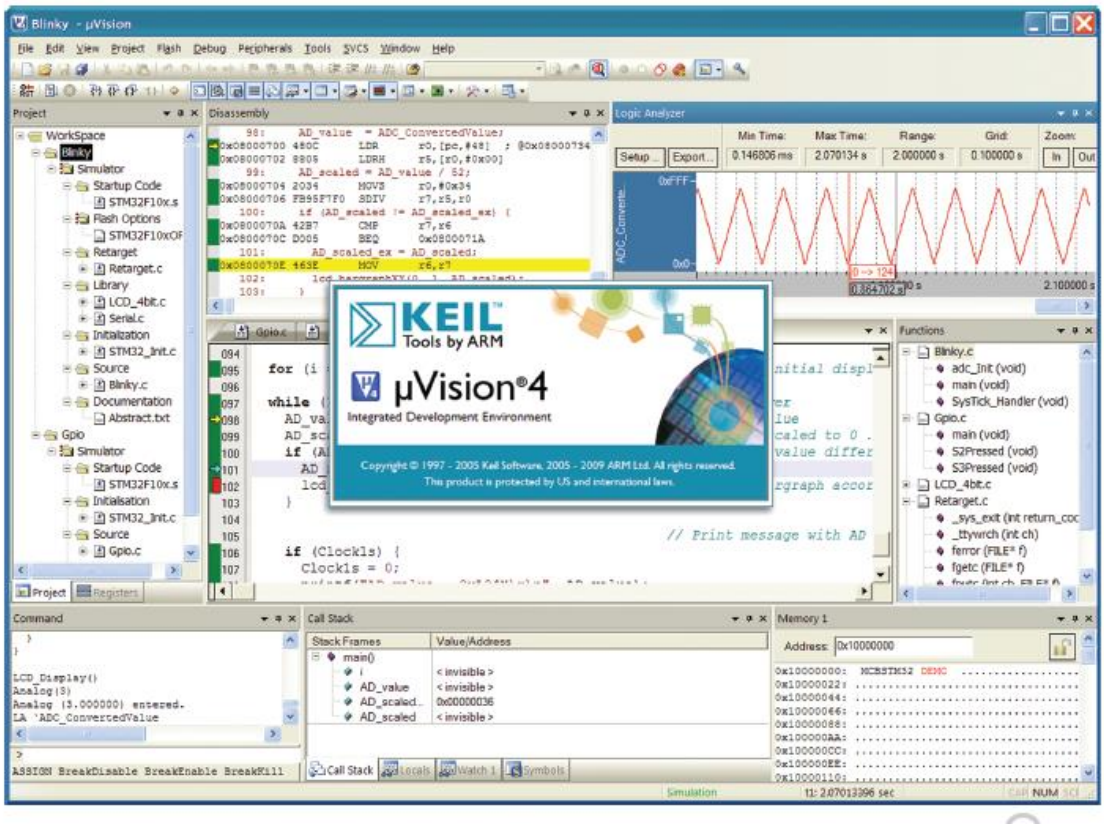

Figure 3.5: MDK version5 developer Environment

3.3.1.1 MDK core

The MDK Core includes all the components that you need to create, build, and debug an embedded application for Cortex-M processor based microcontroller devices. The Pack Installer manages Software Packs that can be added any time to the MDK Core. This makes new device support and middleware updates independent from the toolchain.

3.1.1.2 Software packs

The device packs contain supports for a complete microcontroller family and include system startup code and peripheral drivers. The CMSIS Pack provides Coretx-M core access, an extensive DSP library and a standardized RTOS kernel. The Middleware Pack available in the MDK Professional Edition, includes TCP/IP

networking, USB Host, USB Device, CAN, File Storage, and a graphical user interface library.

3.3.2 What is CMSIS?

The CMSIS enables simple software interfaces to the processor for interface peripherals, real-time operating systems, and middleware. Companies have developed CMSIS driver files for their microcontrollers and you can simply download it from the web site and add to your project. The CMSIS application software components are:

CMSIS-CORE: Defines the API for the Cortex-M processor core and peripherals and includes a consistent system startup code.

CMSIS-RTOS**:** Provides standardized real-time operating systems and enables therefore software templates, middleware, libraries, and other components that can work across supported RTOS systems.

CMSIS-DSP**:** Is a library collection for digital signal processing (DSP) with over 60 Functions for various data types, fix-point and single precision floating-point (32-bit) [58, 59].

3.3.3 µVision IDE

µVision integrates a robust editor, project manager and build facility for efficient software development. µVision IDE combines project management and source code editing capabilities in a single development environment:

Integrated Device Database provides start-up code and tailored peripheral views for a vast array of ARM Powered MCU devices

Editor provides an optimized workflow with intuitive toolbars

Source Browser provides access to all application symbols

Configuration Wizard allows to view, modify, and document bit-level settings quickly and easily [58, 59].

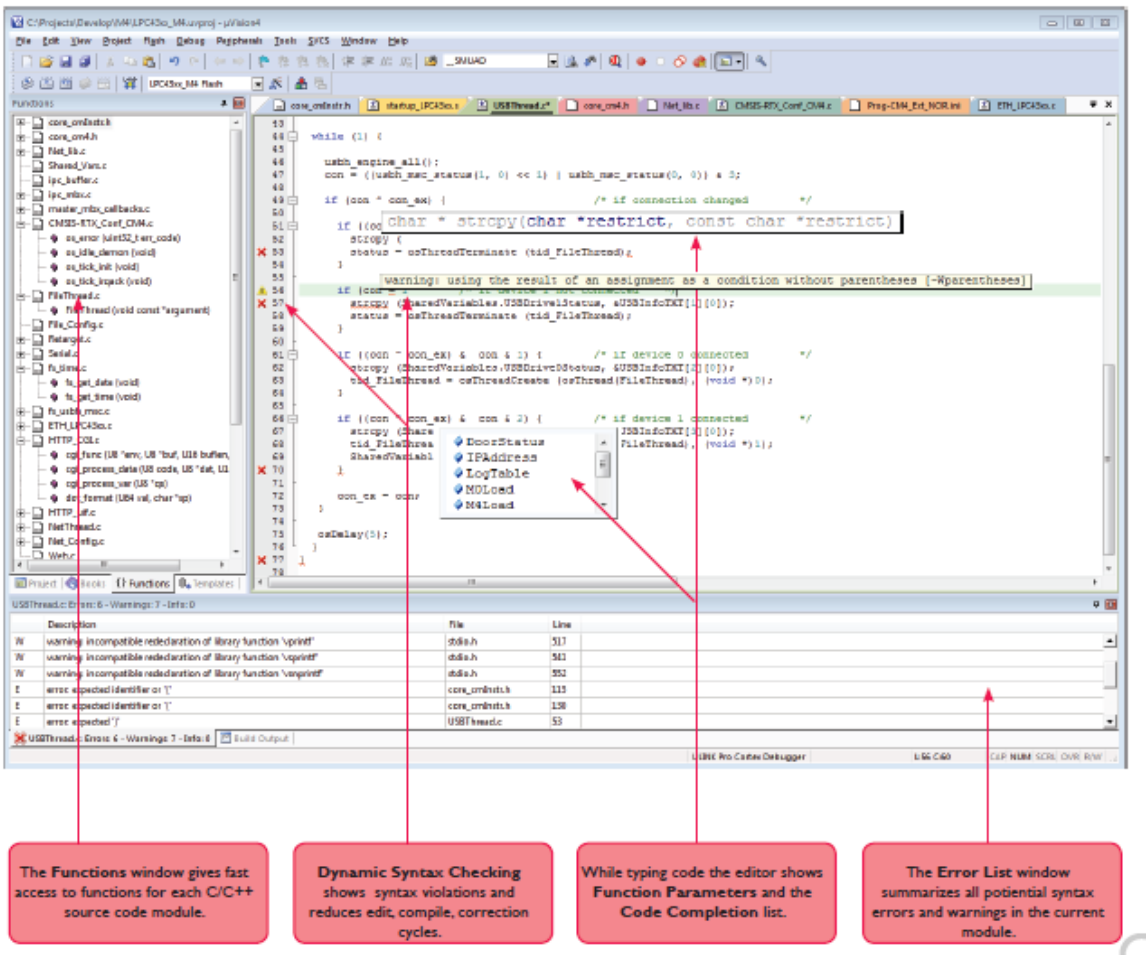

Figure 3.6: MDK version5

3.3.4 µVision Debugger

µVision Debugger provides a single environment to test, verify, and optimize your application and includes:

System Viewer windows display detailed information of peripheral registers. Content values are instantly updated by the target hardware as changes occur.

Logic Analyzer gives a graphical display of signals and variables

Code Coverage statistics verify applications that require certification testing and validation

Performance Analyzer displays the execution time recorded for functions in your application

•**Execution Profiler** records statistics for each CPU instruction, including the execution count and execution time

•**Call Stack** window displays current call nesting with argument and local variables [58, 59].

4 **FIGARO GAS SENSORS**

4.1 Sensors Overview and Applications

Using its innovative gas sensing technologies, Figaro Engineering globally provides cost-effective gas sensing solutions for a wide range of applications in the fields of home and personal safety, industrial safety(instruments like toxic and explosive gas leak detectors, fuel cell leakage detectors, portable gas leak detectors and alarms), air quality control (instrument for VOC monitors for workplace and oxygen monitor for medical usage) , HVAC, home appliances, and the automotive industry. Sensors that are used in this work are TGS 2600,2602,2610,2620 series. The TGS 2600 has high sensitivity to low concentrations of gaseous air contaminants such as hydrogen and carbon monoxide which exist in cigarette smoke. Not only does the TGS 2602 has a very high sensitivity to the air contaminants which are given out by cigarette smoke, but also to low concentrations of odorous gases such as ammonia which is generated from waste materials in office and home environments. Another genre is the TGS2610 which is a semiconductor type gas sensor that is able to combine a very high sensitivity to LP gas which is long life and does not consume a lot of power. Another model that is very sensitive to the vapors of organic solvents in addition to other volatile vapors is TGS 2620. Likewise, It is sensitive to a variety of combustible gases such as carbon monoxide and thus it can be considered as a good general purpose sensor.

4.2 Operating principle

Most typically a metaloxide, SnO_2 is utilized as the sensing material in TGS gas sensor. As a result of heating a metal oxide crystal such as SnO_2 at a certain high temperature in air, oxygen is adsorbed on the crystal surface with a negative charge. After that, electrons acting as donors in the crystal surface are transferred to the adsorbed oxygen, ending in leaving positive charges in a leaving positive charges in

a space charge layer. Thus, surface potential is formed to serve as a potential barrier against electron flow (Figure 4.1)[14].

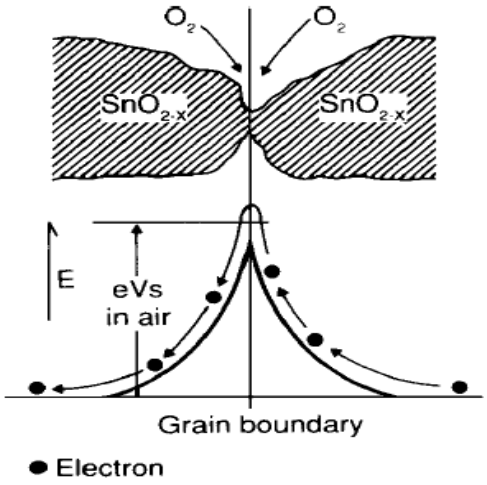

Figure 4.1: Model of inter-grain potential barrier (In the absence of gases)[14]

Inside the sensor there are some conjunctions or so called grain boundaries of SnO_2 micro crystals through which the electrical current can flow At grain boundaries, a potential barriers is formed as the result of the oxygen which has been absorbed that prevents free movement of carriers. The electrical resistance of the sensor is attributed to this potential barrier. Owing to the presence of a deoxidizing gas, the surface density of the negatively charged oxygen decreases, so the height of the barrier in the grain boundary is diminished .As the height of the barrier is reduced, the resistance of the sensor decreases as well. The relationship between the sensor resistance and the concentration of deoxidizing gas can be expressed by the following equation over a certain range of gas concentration [14].

$$R_s = A[C]^{-\alpha} \quad \textbf{(4.1)}$$

Where:
R_s= electrical resistance of the sensor
A = constant
[C] = gas concentration
α = slope of R_s curve

4.3 Sensor Characteristics

4.3.1 Dependency on partial pressure of oxygen

Figure 4.2 illustrates the relationship between the oxygen pressure in the atmosphere (PO2) and the resistance of a typical TGS sensor in clean air. It is important to note that the effect the reduction of oxygen pressure will result in a decline in the sensor's resistance[14].

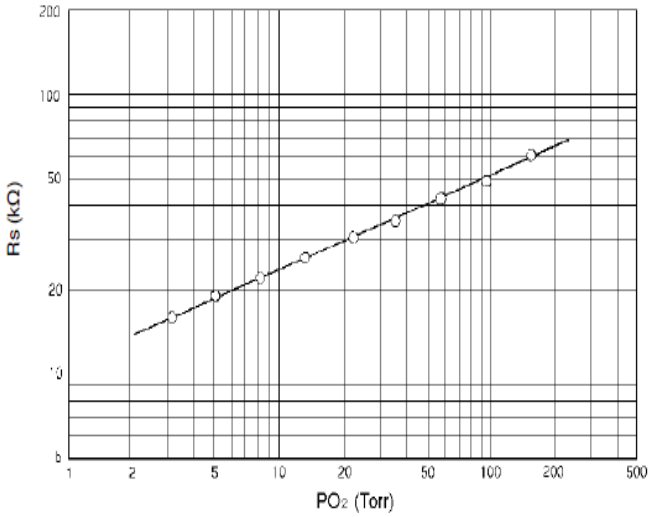

Figure 4.2: Typical dependency on PO2[14]

4.3.2 Sensitivity to gas

According to the given formula in Section 1, the relationship between sensor resistance and gas concentration is linear on a logarithmic scale presuming a practical range of gas concentration (from several ppm to several thousand ppm). The sensor will be sensitive to different kinds of deoxidizing gases and it is relatively sensitive to certain gases that are optimized by the formulation of sensing materials and operating temperature. Insomuch the actual values of sensor resistance are variable from a sensor to another, for expressing the typical sensitivity characteristics a ratio of sensor resistance in various concentrations of gases (Rs) over resistance in a certain concentration of a target gas (Ro) are taken into account[14].

4.3.3 Sensor response

The typical behavior is demonstrated in Figure 4.3first when the sensor is exposed to and then it is removed from a deoxidizing gas. The resistance of the sensor will tumble down very quickly at the time of exposure to a gas, and when it is removed

from the gas, its resistance will regain its original value after a short time. On the basis of the model of sensor and the gas involved the speed of response and reversibility will modify[14].

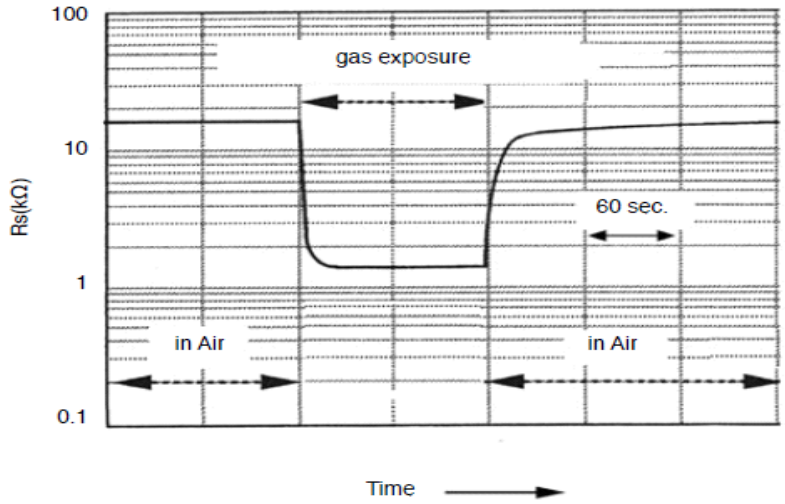

Figure 4.3: Typical sensor response[14].

4.3.4 Initial action

As depicted in Figure 4.4 all sensors reveal a transient behavior which is referred to as "Initial Action" when stored unenergized and later energized in air. The Rs collapses sharply immediately after the first few seconds while energizing, regardless of the presence of gases, and then it reaches a stable level in accordance with the ambient atmosphere. The atmospheric conditions during storage are effective in determining the length of initial action and the length varies by sensor model. Contemplation of this behavior is necessary while designing a circuit because it may cause the activation of an alarm during the first few moments of powering[14].

4.3.5 Dependency on temperature and humidity

The principle of detection of TGS sensors is based on the chemical adsorption and desorption of gases on the sensor's surface. Accordingly, the sensitivity characteristics will be affected by the ambient temperature as the rate of chemical reaction is changing. In addition, humidity causes a reduction in Rs when water vapor adsorbs on the sensor's surface. A typical example of these dependencies is shown in Figure 4.5. Consideration of a compensation circuit for temperature dependency is required while using TGS sensors [14].

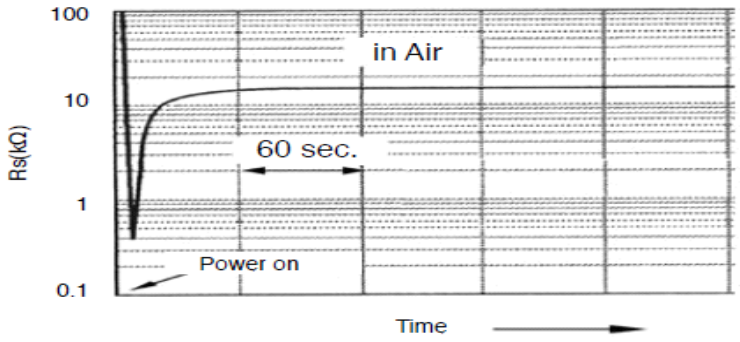

Figure 4.4: Typical initial action[14].

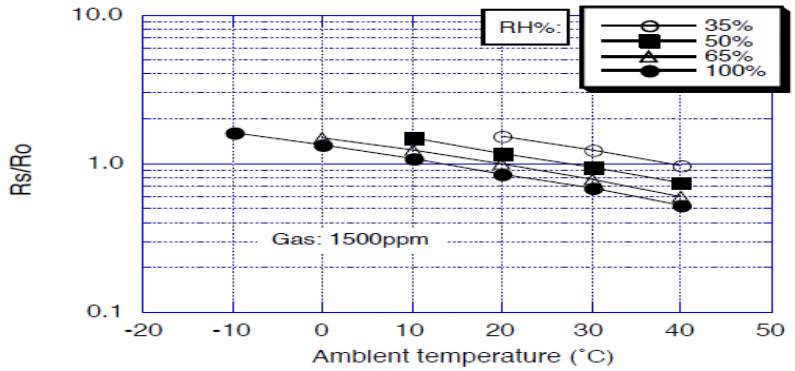

Figure 4.5: Typical temperature and humidity dependency [14]

4.3.6 Long term stability

Figure 4.6 shows typical data of long term stability for TGS series sensors. Commonly, TGS sensors reveal stable characteristics over time and due to this they are found to be suitable for maintenance-free operation[14].

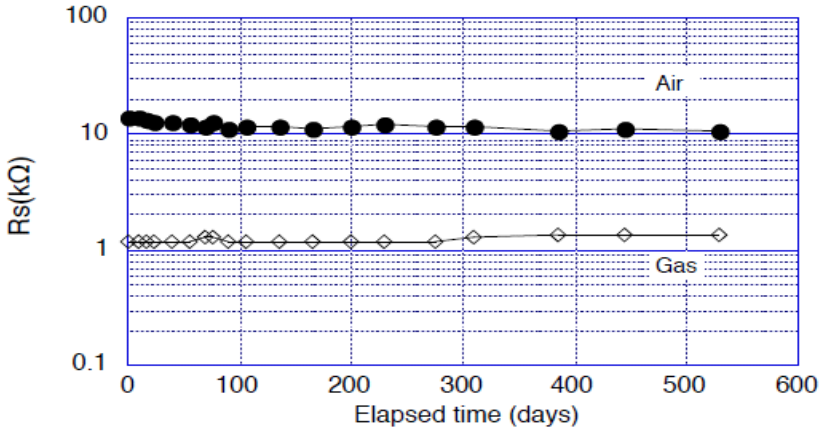

Figure 4.6: Typical long term stability [14].

4.4 Circuit Design

4.4.1 Load resistor (RL)

Through the RL the output signal can be obtained acting as a sensor protector .It regulates the sensor power consumption (Ps) below the rated value for the sensor. On the condition that the RL is being selected appropriately for an individual sensor, the sensor will be able to provide identical characteristics so that users can apply the sensor under the best circumstances[14]. Meanwhile, Figure 4.7 shows the gas concentration versus the output voltage (VRL) when the sensor and various RL values (5kΩ, 2.5kΩ, 1kΩ) are used in a circuit along with each other simultaneously. Figure 4.8 shows the relationship between Rs/RL and VRL/Vc. At the point where Rs/RL is equal to 1.0, the slope of VRL/Vc soars up to its maximum. This is the point where the optimal resolution of signal at alarm concentration can be obtained. As a result, it is proposed to use an RL whose Rs/RL value is equal to 1.0 at the concentration to be detected. To gain the optimum results, a variable resistor (RL) is suggested[14].

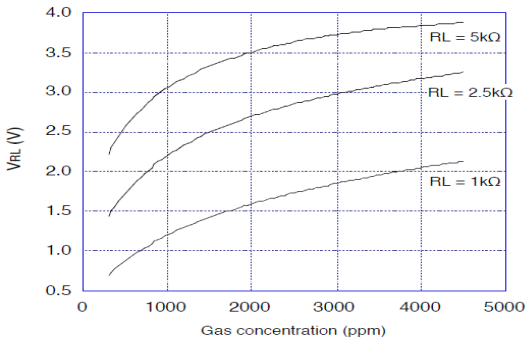

Figure 4.7: Sensitivity characteristics (VRL)[14]

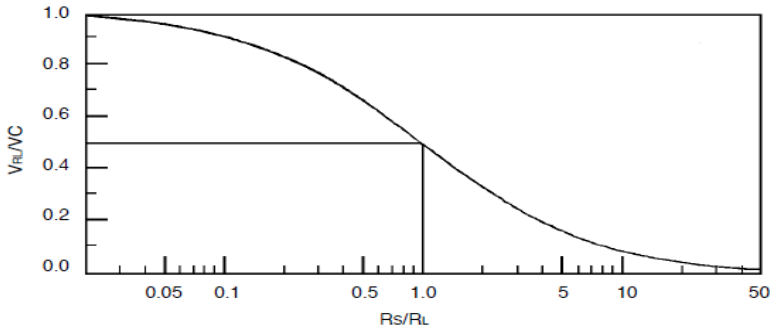

Figure 4.8: Relationship between Rs/RL and VRL/Vc[14

4.4.2 Basic measuring circuit

Structure and dimensions of 2600 series are shown in figure 4.9.

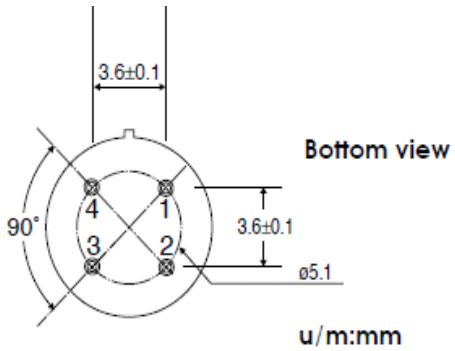

Figure 4.9: The Figaro sensor Pin connection:[14]

1: Heater
2: Sensor electrode (-)
3: Sensor electrode (+)
4: Heater

Two voltage inputs are needed for the sensor: heater voltage (VH) and circuit voltage (VC). The heater voltage (VH) is applied to the integrated heater in order to maintain the sensing element at a specific temperature which gives the optimal results for sensing. The circuit voltage (VC) is applied to allow measurement of voltage (Vout) across a load resistor (RL) which is connected in series with the sensor. A common power supply circuit can be used for both VC and VH to accomplish the sensor's electrical requirements. For the optimization of the alarm threshold value, the value of the load resistor (RL) ought to be selected meticulously in a way that the power consumption (PS) of the semiconductor is retained below the limit of 15mW. Power consumption (PS) will be at its highest quantity so long as the value of Rs is equal to RL while being exposed to a gas.

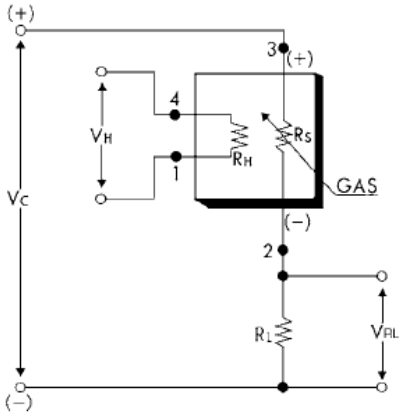

Figure 4.10: Sensor resistance (Rs)[14].

If the measured value of Vout is given, then sensor resistance (Rs) can be calculated according to the following formula:

$$R_S = \frac{V_c \times R_L}{V_{out}} - R_L \qquad \textbf{(4.2)}$$

Meanwhile, the value of power which is consumed (PS) can be calculated if the following formula is used[14] :

$$P_S = \frac{(V_c - V_{out})^2}{R_S} \qquad \textbf{(4.3)}$$

4.4.3 Designed sensors PCB board

PCB board has 4 Figaro gas sensors, 13 resistors and 4 capacitors. The structure of sensors was examined previous sections. If the structure of the sensors are contemplated structure and by using the information on datasheets, a schematic PCB board can be devised for sensors as follows.

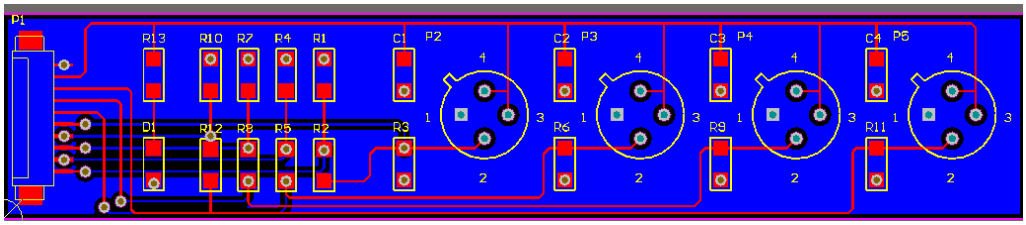

Figure 4.11: PCB of sensors.

R1, R2, … , R13 = 10 Kohm.

C1, C2, C3, C4= 100 pF

The R11,R9,R6,R3 resistors used for pulling down the analog output of the sensor, it means that when there is no voltage the output for the sensor always remains 0 volts .The R1, R2, R4, R5, R7, R8 are used as voltage dividers. As resistors values are the same, the output voltage is divided by 2. The C1, C2, C3, C4 capacitors are used to eliminate noise of the whole circuit. Figure 4.13 shows the designed circuit schematic. Also figure 4.12 illustrate the photo of designed sensor board.

Figure 4.12: Photo of designed sensor board.

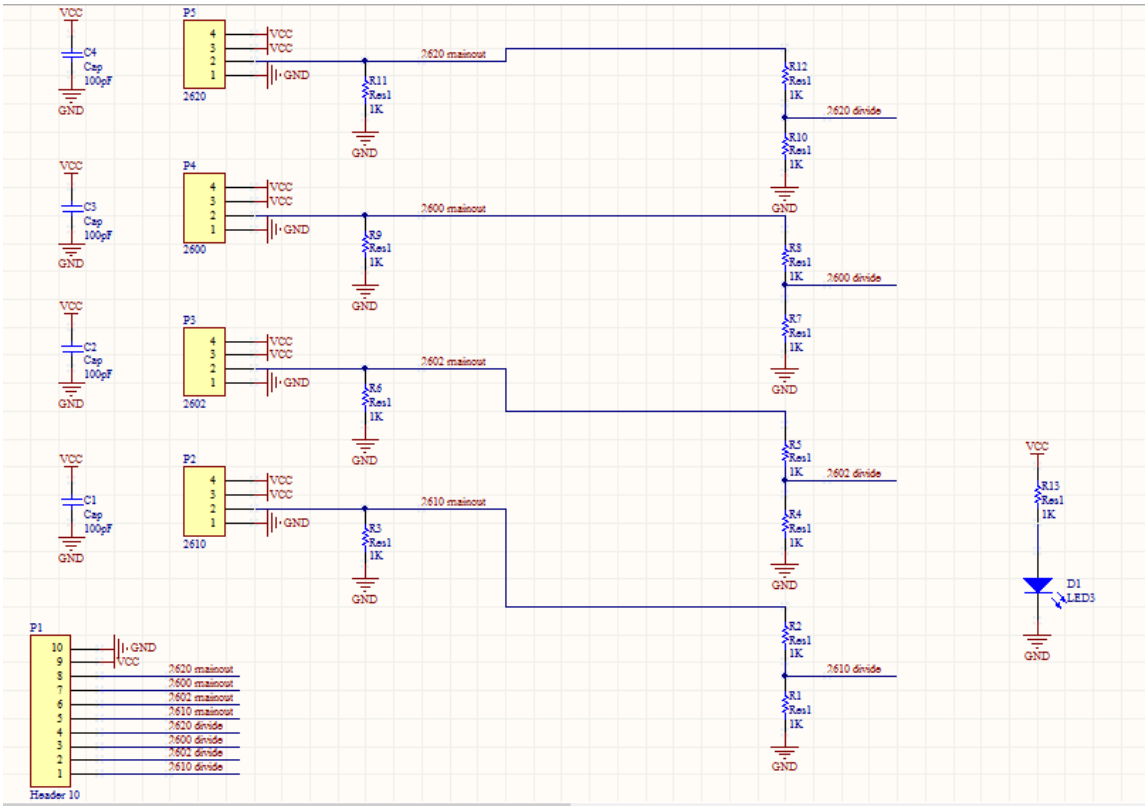

Figure 4.13: Designed circuit schematic of sensor board.

5 THESIS SOLUTION

In this section we want to fulfill the theories which have been mentioned in the previous sections. The systems hardware and board has been studied and reviewed in Chapter 3. Sensors have been driven precisely and then are connected to the microcontroller. In this case, we can start to test circuits and written algorithms. To perform the test, we have considered a package or box that can be fully brought into fresh air or can be filled by our considered gases. For testing, we have considered two approaches:

- Test smoke cigarette
- Test by spraying alcohol that produces ethanol odor

At the end of this section, we want to measure the correct values of the gases in the air by the performance and implementation of the algorithms.

5.1 How to Get Database

There are several ways to get the raw data, which was not possible for us to implement some of these methods. These methods included:

- Measure input gas and applying it to a sensors and measuring output of each senor for the specified input gas.
- refer to the technical data sheet of sensors and extracted raw data

The approach that we use to obtain raw data for training neural network is the latter choice. The reason for using this method is the lack of measurement devices that gives accurate knowledge of the sensor output to the specified input gas. In datasheet there are graphs that shows input gas values ratio to Rs / Ro value, that by using this graphs, we can extract the relationship between sensor’s outputs value to input value.

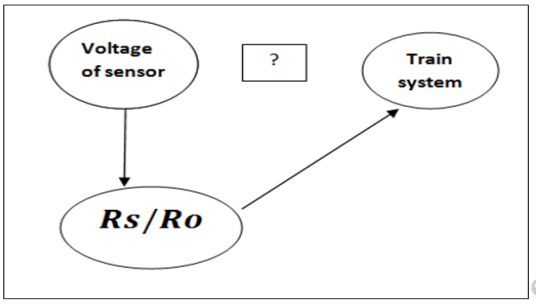

Figure 5.1: Diagram of how to get database values.

By considering figure 4.10 in chapter 4, because R_l value is determined by our own choices, we can realize the current *(I)* values of resistance by measuring the output voltage of sensor.

$$I_{circuit} = \frac{V_c - V_{sensor}}{R_l} \quad \textbf{(5.1)}$$

This is just the total current of circuit. By considering R_s and R_l definition as below:

- Rs: Sensor resistance in displayed gases at various concentrations.
- R_o: Sensor resistance in fresh air.

The internal resistance of sensor in fresh air (R_o) and in gas concentration (Rs) can be calculated as below:

$$R_s = \frac{V_{sensor}}{I_{circuit}} \quad \textbf{(5.2)}$$

$$R_o = \frac{V_{sensor}}{I_{circuit}} \quad \textbf{(5.3)}$$

And finally by dividing $R_s\ to\ R_o$, we earn the value that graphs of input gas to output is plotted based on. According to graphs of datasheet, the ethanol gas has been selected as reference gas, and dataset have been generated based on. Since graphs can be assumed linear, we can obtain the R_s / R_o value and record it. From each graphs, approximately 40 parameters can be extracted as database. In some cases, relationship between Rs / Ro value and output of sensor is not proportional. For example 2610 sensor series, so datasheets gives a formula (5.4) to correct it. We program the formula in micro and consider datasheet graph as our dataset.

$$\text{Rs / Ro} = \text{measurement/1800 PPM} \quad \textbf{(5.4)}$$

Dataset tables that extracted from datasheet are given in appendix 2.

5.2 Possible Errors:

Errors in our system cause by 3 important factors. The first one is measurement errors. For measuring output voltage of sensors, the ADC of microcontroller needs to be implemented. Measuring output voltage of sensors by ADC brings a kind of error that it is about 2 LSB according to datasheet references. It means that if measuring voltage be converted to digital number by 12 bit resolution, two LSB Bits contains error. For eliminating this error we can remove or ignore two least bits that contain error. By removing these two bits our accuracy in measurement of output voltage of sensor will be reduced. So we have 2 options:

- Accepting output of sensors by high accuracy and 2 LSB error
- Removing error and measuring voltage of sensor by diminished accuracy

According to experience and testing of available options, the first option is more acceptable and appropriate, so in this work, we select the first choice. The second general error is related to algorithms. This means that when we choose an algorithm to apply on input data, the algorithms reliabilities is not adequate and contains a range of errors. Last general error belongs to our database. This kind of error appears when we collect our data base. For example when we measure our outputs according to our inputs, the output value that we recorded may be not the exact number of corresponding input value. All three major forgoing errors added together and effect system. Despite of all, the outcome result errors always are below the 10% that is acceptable value.

5.3 How Implement Algorithms in Practical Way:

5.3.1 KNN:

The KNN algorithm as discussed before is based on difference concept. We can assume algorithms in 2 ways:

- Linear
- Euclidean

In this work we accepted the first assumption, since relation between our input databases is linear. If input value that we earn from sensors was the same as our database value, the algorithm consider database output as correct output and this

value will be displayed on LCD. Otherwise we implement algorithm by computing the distance between input values and applying it to output value. In this solution, if the value of input which has been obtained by microcontroller was between range of two numbers of our database inputs, and by assumption that data changes in linear way, we can calculate the distance between inputs and then interfere this value by output value of database. The answer is our considered output. The method is clarified by an example as below:

For instance if the input value that is obtained by micro be 1.08, and our database table is as figure 1, so the number is between 2 database values.

Input $(\frac{R_S}{R_o})$	1	1.2
Output(PPM)	100	105

1 ← 1.08 → 1.2

Figure 5.2: Example dataset.

Firstly, calculate the distance between two input numbers, here the distance between 1 and 1.08. It is 0.08 in this example. And again calculate the distance between database input values that is 0.2. Then the percentage of vicinity between numbers can be obtained as below:

$$x = (100 \times 0.08)/0.2 = 0.4 \quad \textbf{(5.5)}$$

Figure 5.3 clarifies calculation process. In next step the distance between two corresponding output values of database should be calculated and then be multiplied by the percent of previous stage value.

$$105 - 100 = 5 \quad , 5 \times 40\% = 2 \text{ and } \quad 100 + 2 = 102 \quad \textbf{(5.6)}$$

The output value that is obtained by KNN algorithms is 102 for input value that was 1.08. The stages can repeated for two other pairs of dataset, and the vicinity percent can be calculated, the same result will be obtained.

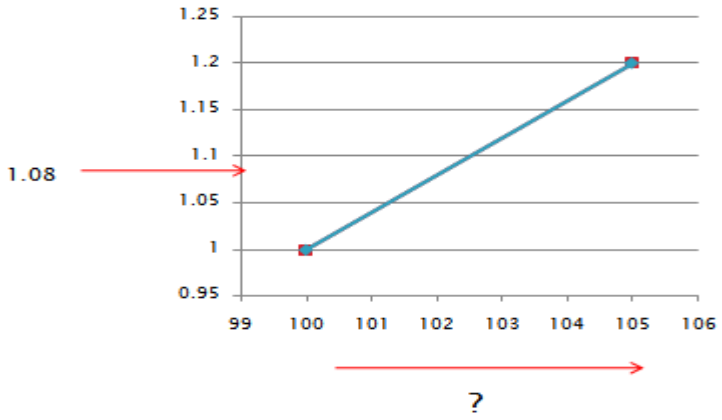

Figure 5.3: Graph of example dataset.

5.3.2 MLP:

In this method firstly the system should be trained by the input values and MLP algorithms. Matlab program is selected for training our system. Training process will be explained in coming sections. In this system, we have 4 input values from sensor; algorithms should be applied for each input separately. For each input, we assume two hidden layers and 10 neurons. The block diagram is as Figure 5.4. In first stage, the output of hidden layers can be computed by multiplying input value in each of weights. Here the multiplying process should be repeated for 10 times, since 10 neurons be assumed for system. In second stage, we use sum function to add all multiplied values. And in last stage, the value from second stage is applied to sigmoid function (eq.5.7).

$$\delta(x) = \frac{1}{1-e^{x}} \qquad \textbf{(5.7)}$$

The output of this stage is answer of system to MLP algorithms and can be displayed on

LCD. This process is implemented for each sensors and the result is displayed separately.

5.3.2.1 Matlab training:

Matlab Neural network toolbox is used to train the system. As explained before, Weights and biases that are achieved from Training part, will be used by MLP algorithm in this thesis. So the goal here is to find weights and biases from training network.

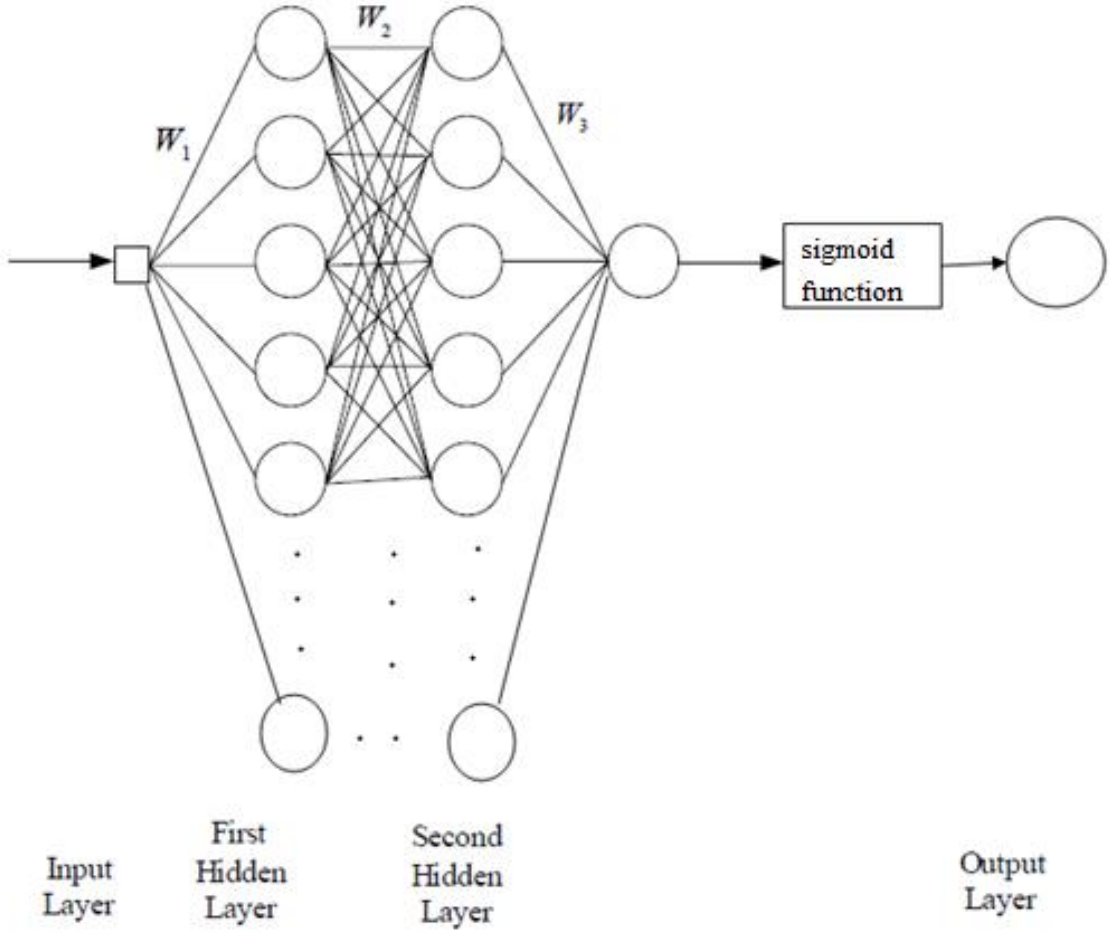

Figure 5.4 Block diagram of neural network.

How to get dataset samples from datasheet has been explained in previous section. Database values will be used as input and target values in training process. We use Graphical User Interface of neural network that is simple and easy to use. I review a Brief explanation of training process as below:

In first step we create input and target matrices and copy data into them in workspace, Then in second step we type ‘nntool’ or ‘nnstart’ in command window. nntool opens the Network/Data Manager window, which allows you to import, create, use, and export neural networks and data. Now we can Import input and target values into Data Manager Window. In the next step by clicking on ‘new’ option, Create Network or Data window will be appear. In this dialog box we can adjust network properties like training function, number of layers and other factors. Then by clicking create, the network will be created. Now we can Train the network. Figure 5.5 shows training dialog box. Then training parameters can be change as shown in figure 5.6.

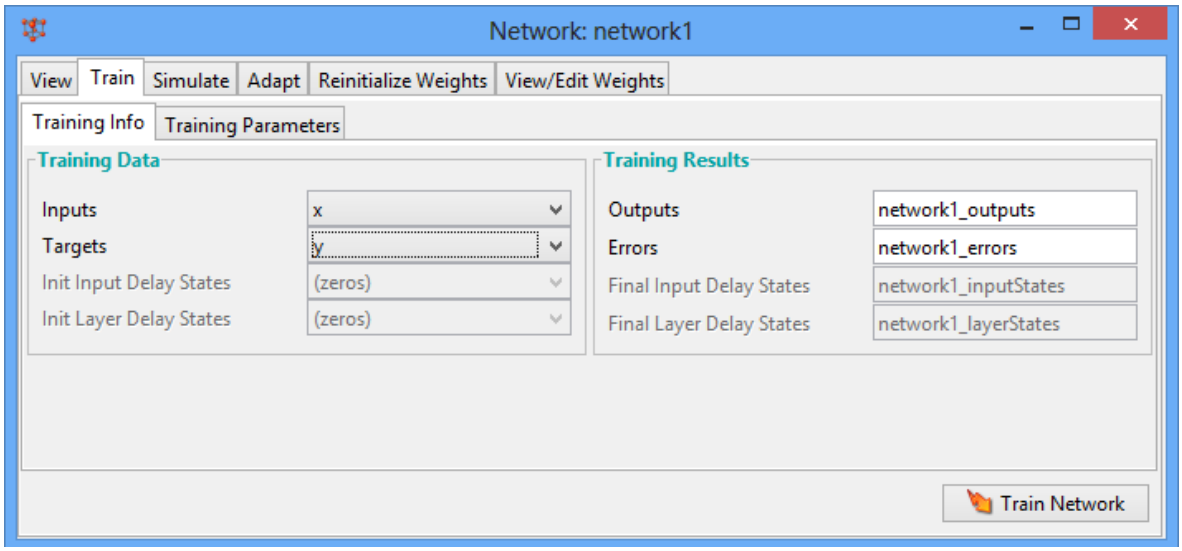

Figure 5.5: Created network training dialog box.

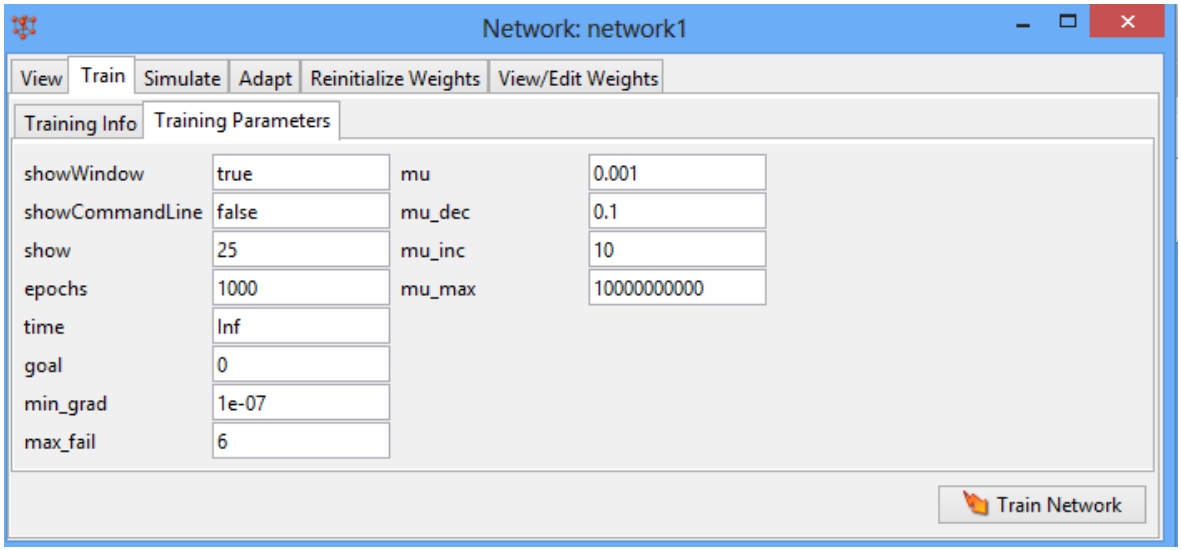

Figure 5.6: Parameters in training window.

After training the network, we consider performance plot to know best performance as illustrated in figure 5.7 and 5.8.

In final step we Export all data to Matlab workspace. Now network1.LW and network1.IW commands returns network weights. Typing network1.b also will give biases values [50, 51].

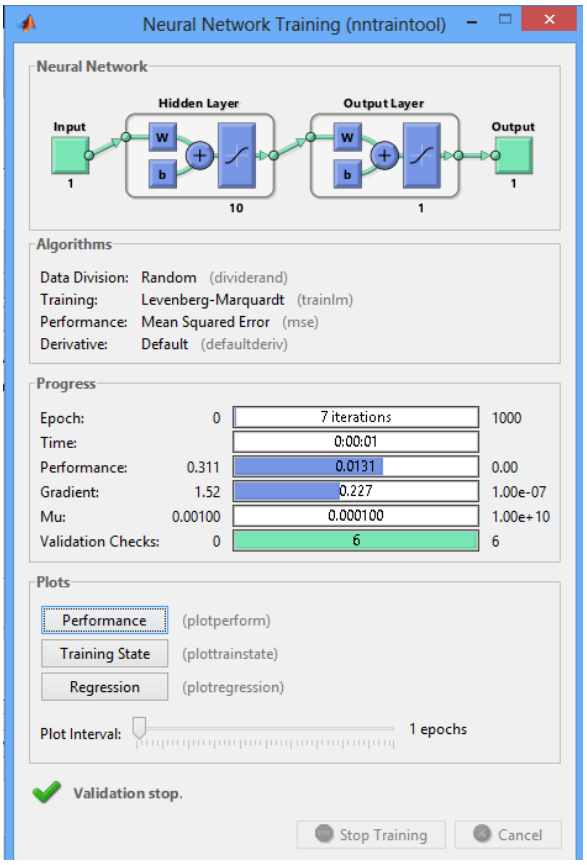

Figure 5.7: Neural network training

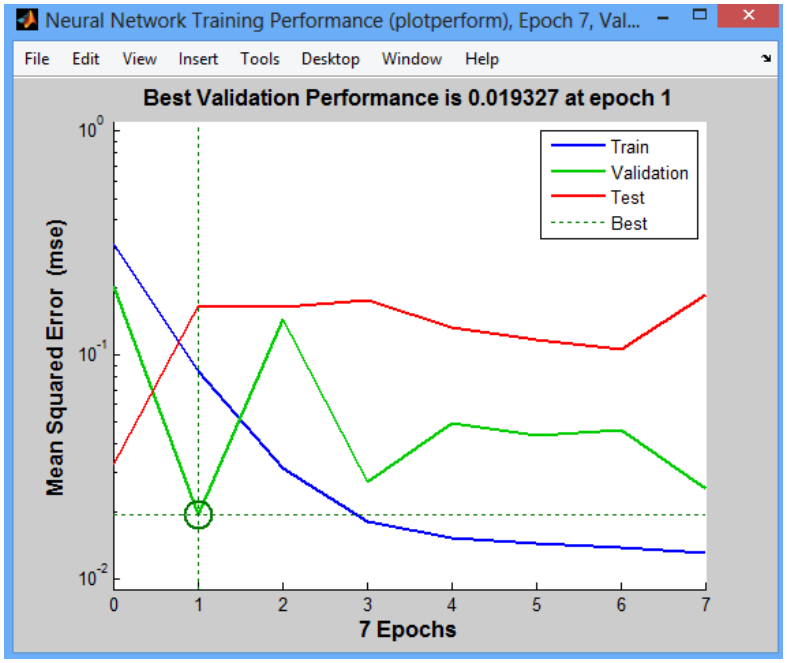

Figure 5.8: Neural network training performance window

5.3.3 PCA :

This algorithm is more popular when the number of input data is huge and bulk. Imagine that input values are collected in matrix, the matrix dimension is 100 * 100. In this case for decreasing the mass of input data without loss of accuracy, The PCA algorithm can be used. For example, suppose a 100 * 100 matrix, for decreasing the content of matrix, In first step Covariance of matrix should be calculated. If we needed 3 PCA factors, the output of covariance should be 100* 3 matrix. Then in second phase the input primary matrix must be sorted. In this work bobble sorting method is implanted. Data sorted by bobble sorting method is in min to max order. In third phase sorted matrix is multiplied in covariance matrix of stage one. The answer that earned from third stage is 100 *3 matrixe that has the features and attributes of 100*100 matrix. The dimension is decreased but the features are the same, only a little error occurs. The PCA first and second and third components then can be used by other algorithms such as KNN or MLP. In this work component of PCA are used by KNN algorithm.

5.4 Accuracy of Algorithms:

To ensure the accuracy of algorithms in this work, for each of algorithms, we consider input and study their corresponding output. For instance imagine KNN algorithm, without connecting sensors and by a simple code, we generate a series of new inputs, like our database input values, then we applied this inputs to KNN algorithm, in this case we anticipate displayed output on LCD be proportional to database outputs. So we generate a string of data randomly, by 1 ms interval we applied data values to written algorithm and record the output values. Then try to add data in table and plot the diagram. By comparing new diagrams and dataset diagram, we attain the point that our written algorithms work probably. For each of algorithms, we connect the sensors one by one, in first step expose sensor in fresh air, then in second step expose sensors in concentration of gasses that caused saturation. We save the output value of sensors and record it as max and min value. Then we applied these values (max and min) to algorithm, and save the output. By comparing between this data with our database min and max value, the error of

algorithms can be obtained as it explained before. In each of KNN and MLP and PCA algorithms, errors are below 10%.

5.5 Experiment and Result

Two scenarios are designed to testing algorithms. In first scenario we choose alcohol for test. We pour liquid alcohol to spray. By using spray in fact we broken the alcohol to tiny drops and it is like we strew the alcohol in fresh air. The times that we push spray is important factor here. In second scenario the smokes of cigarette is testing material that contains CO2 gases. For evaluation output of sensors, first we applied one lighten cigarette in closed box for 5 second, then we bring it out. We repeat this test for 10 second and continued process until 50 second. In next turn we applied 2 cigarettes in box, then bring them out and continued test by 5 second intervals, repeat process until sensors reach their saturation point. We use these two scenarios, since we did not have access to gas measurement devices that gives the concentration of gasses.

We start testing by KNN algorithm. KNN algorithms can be selected by pressing key on microcontroller board. Then we started to apply scenarios. In first step, we spray ethanol gas in package, and then we put sensors in package, and try to plot the output of each sensor. Then we allow sensors to be in fresh air and return to their fresh air vales. This time is approximately 4-8 second and depends on density of gases in package. In second step, after discharging previous gases, again we spray ethanol but two times and put sensors in package and plot the graphs. Again we bring out sensors and let them to be in fresh air. In third step after discharging previous gases, we spray ethanol but three times and then we put sensors in package and again try to plot graph. We continue this process until sensors reach their saturation point. Diagrams of first scenario are as Figure 5.9.

There are some points here. First, some sensors like 2600 series, reach their saturation point before others. The reason for this goes back to how it's designed and built to measure gas with low concentrations. In this case we should ignore the sensors that reach their saturation point, because their data is not valid. The second point is that Figaro gas sensors are really sensitive to moisture and humidity. This point should be noticed when we spray ethanol and be careful to avoid direct contact

of ethanol drops by sensors. Also the concentration of gases should be in level that does not damage sensors.

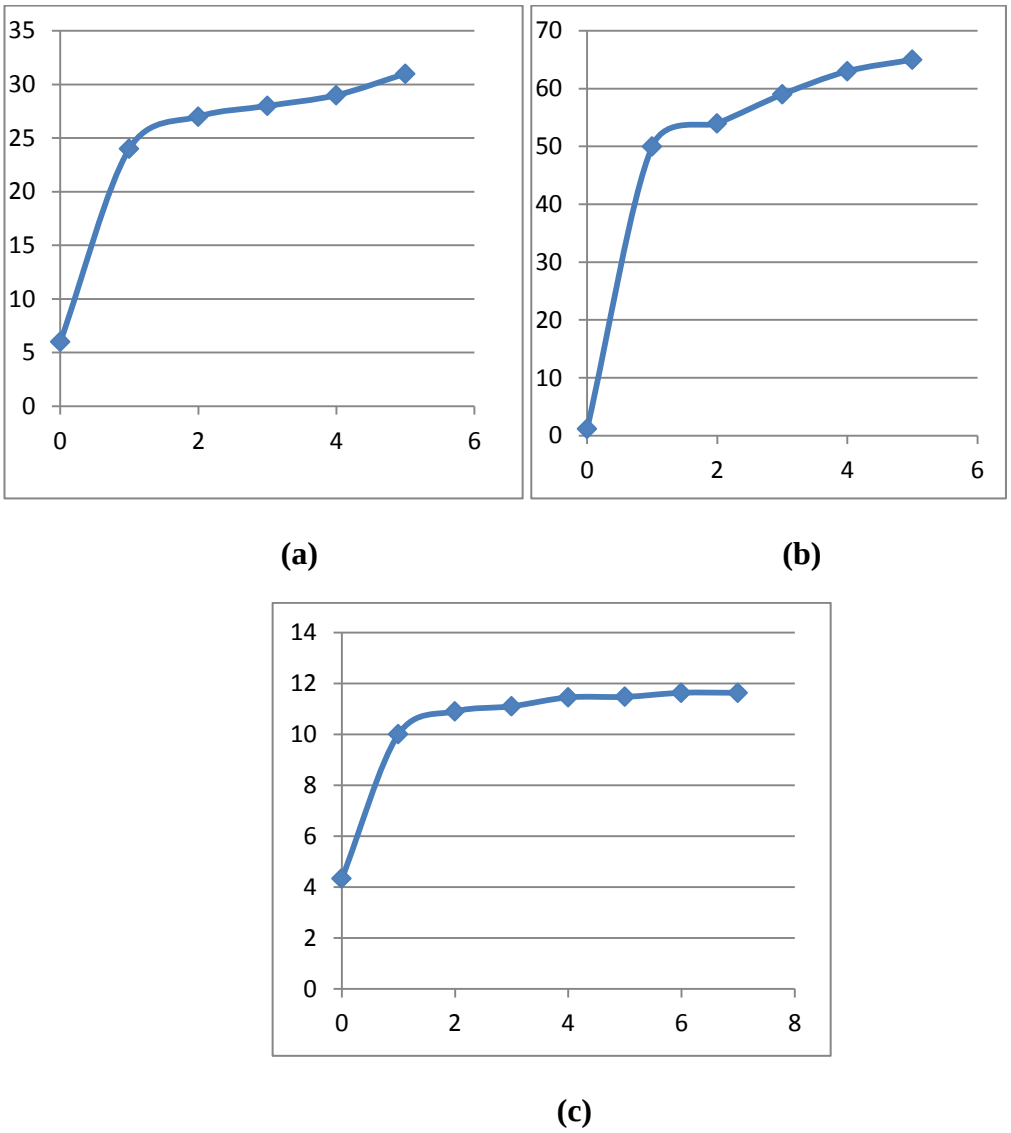

Figure5.9: (a) TGS 2602, (b) TGS2600 and (c) TGS 2620 sensors response to alcohol test (KNN algorithm).

In this scenario again test takes place in closed package. First we light a cigarette and let it well being ignited. Then we put it in a closed environment for 5 second. Then taking the cigarette out and put the sensor in a closed package. In this step we record the values that are displayed on LCD and plot the graphs by EXCEL program. Again we let the box be free from smoke of cigarette until the output of sensor shows fresh air values. In third step we repeat two previous steps but by 5 second intervals, we iterate the stage until 50 second by one cigarette then we add second cigarette and

repeat it by 5 second intervals until the sensors reach their saturation point. After collecting data, we draw graphs by EXCEL program. Diagrams are as below:

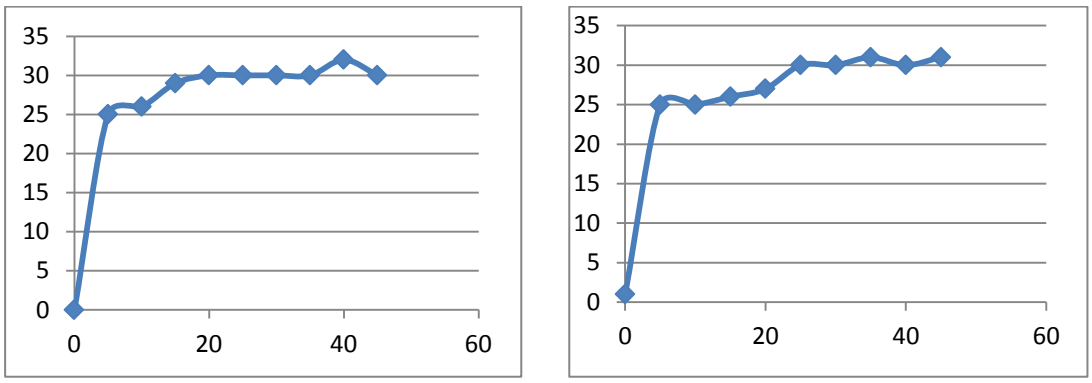

(a) **(b)**

Figure 5.10: TGS 2602 sensor response to KNN algorithm (a) to 1 cigarette test and (b) to 2 cigarette test.

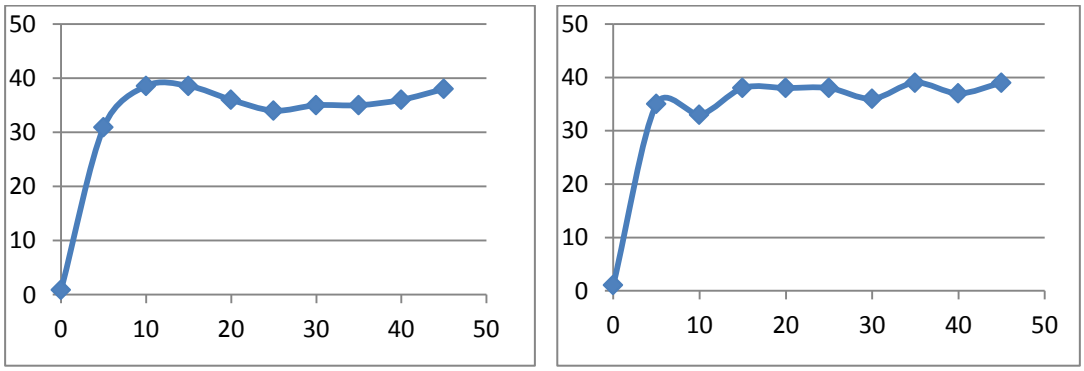

(a) **(b)**

Figure 5.11: TGS 2600 sensor response to KNN algorithm (a)1 cigarette test and (b) 2 cigarette test.

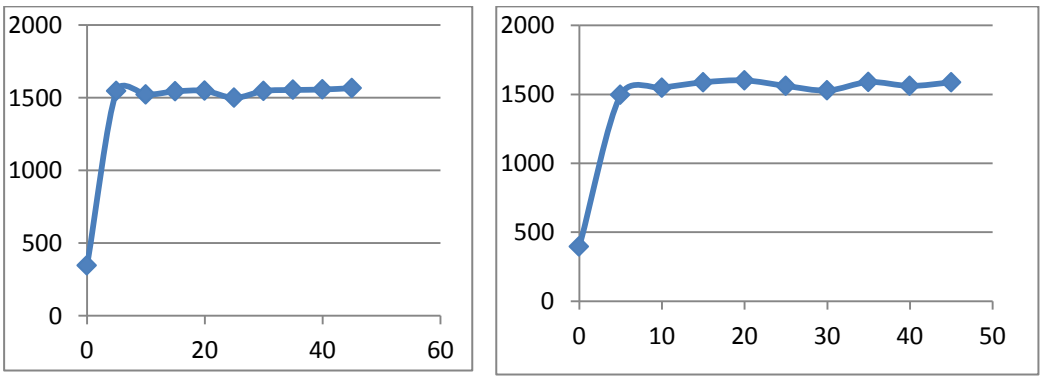

(a) **(b)**

Figure 5.12: TGS 2620 sensor response to KNN algorithm (a).1 cigarette test and (b).2 cigarette test.

The important point in this scenario and previous one that should be considered is that the values of concentration that is measured by sensors depend on dimension. So we should select one standard package during whole of tests.

Another principle point that should be considered is about gas concentration measuring instrument. If such instrument be available and all tests be repeated again, algorithms are the same and fix without any change or defect. The only benefit of device is ability to generate our set of database in closed box and calibrate sensors without need to database that is extracted from datasheet. By this way we can remove the measurement error and database error from performance of algorithms.

We iterate this process for other 2 algorithms as below, First we select the MLP mood by the pressing the key on board and apply two scenarios of smoke and ethanol gas and record values. Diagrams that are earned by applying first scenario in MLP algorithm are as below (test by alcohol):

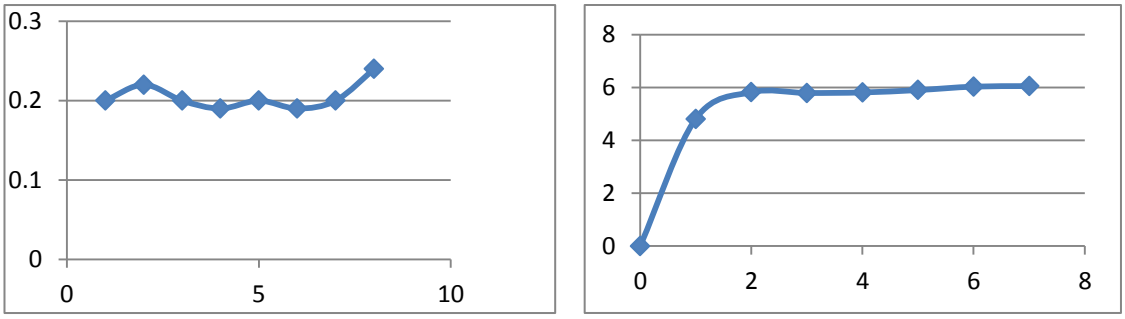

(a) (b)

Figure 5.13: Sensor response to alcohol test in MLP algorithm (a) TGS 2610 sensor and (b) TGS 2602 sensor.

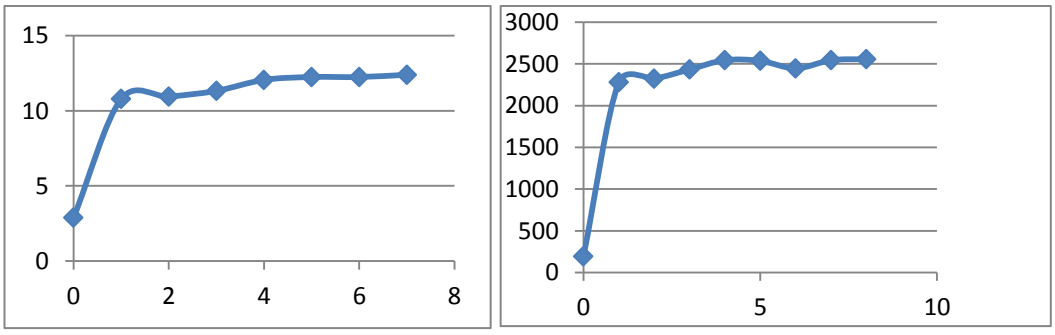

(a) **(b)**

Figure 5.14: Sensor response to alcohol test in MLP algorithm, (a) TGS 2600 sensor and (b) TGS 2620 sensor.

Diagrams that are earned by applying second scenario and MLP algorithm are (test by cigarette) as below:

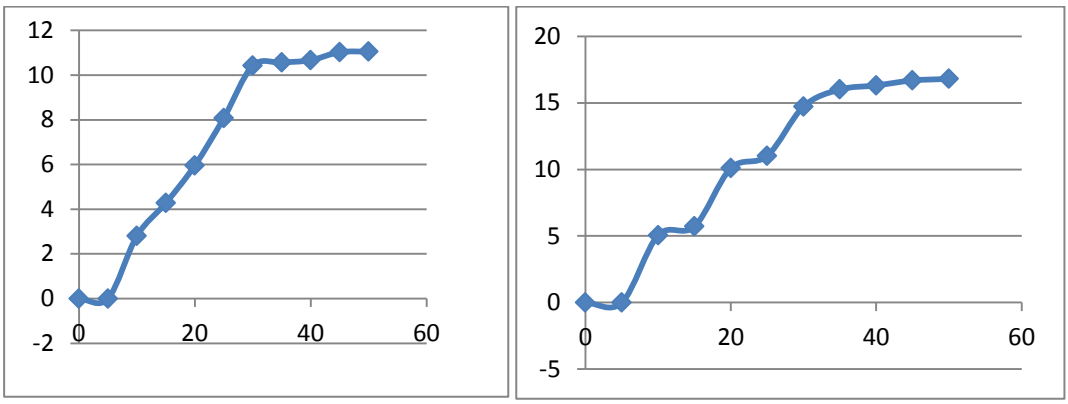

(a) **(b)**

Figure 5.15: TGS 2602 sensor response to MLP algorithm, (a) 1 cigarette test and (b) 2 cigarette test.

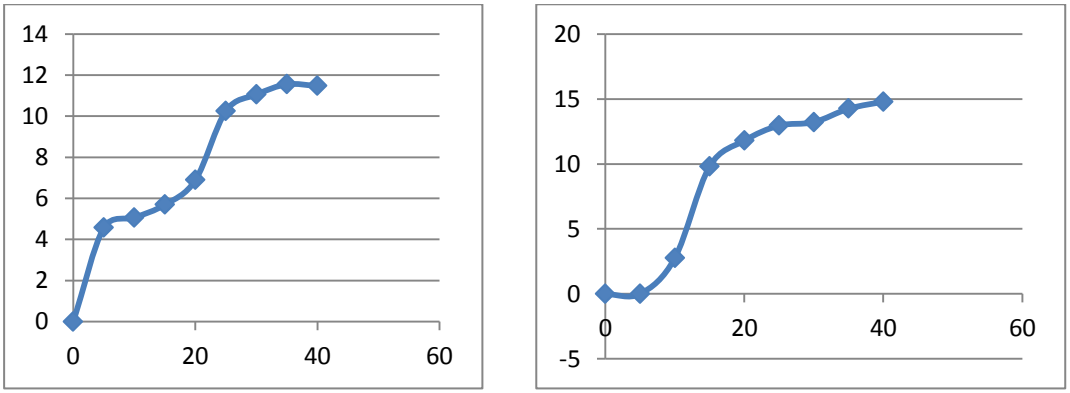

(a) **(b)**

Figure 5.16: TGS 2600sensor response to MLP algorithm, (a) 1 cigarette test and (b) 2 cigarette test.

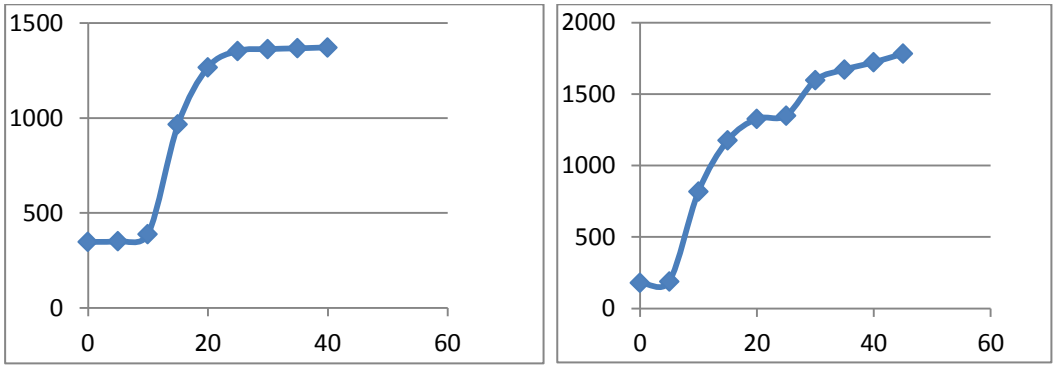

Figure 5. 17: TGS 2620sensor response to MLP algorithm (a) 1 cigarette test and (b) 2 cigarette test.

Then we choose PCA mood and implement two scenarios, record values and plot the graphs by Excel program. Diagrams that be achieved by applying first scenario and PCA algorithm (test by alcohol) are as below:

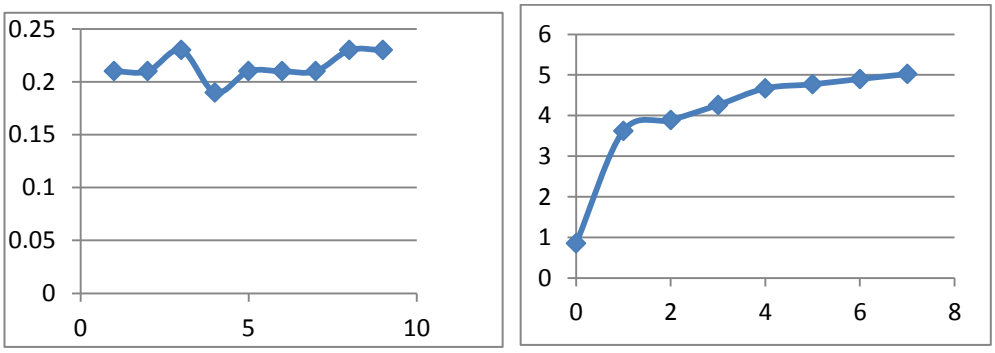

(a) **(b)**

Figure 5.18: Sensor response to alcohol test in PCA algorithm (a) TGS 2610 sensor and (b) TGS 2602 sensor.

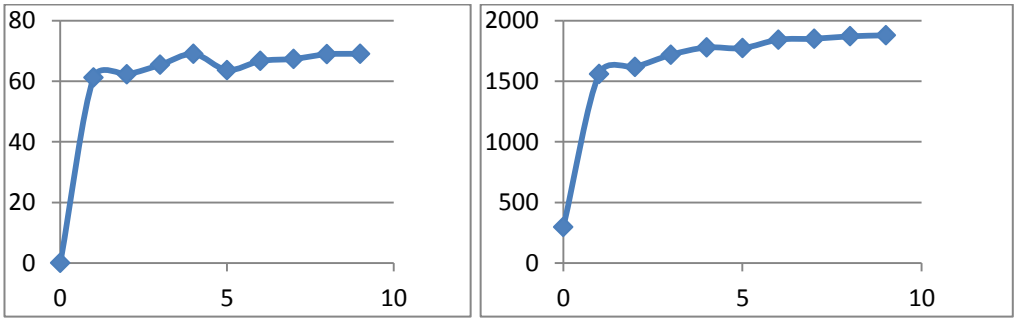

Figure 5.19: Sensor response to alcohol test in PCA algorithm (a) TGS 2600 sensor and (b) TGS 2620 sensor.

Diagrams that be achieved by applying second scenario in PCA algorithm (test by cigarette) are as below:

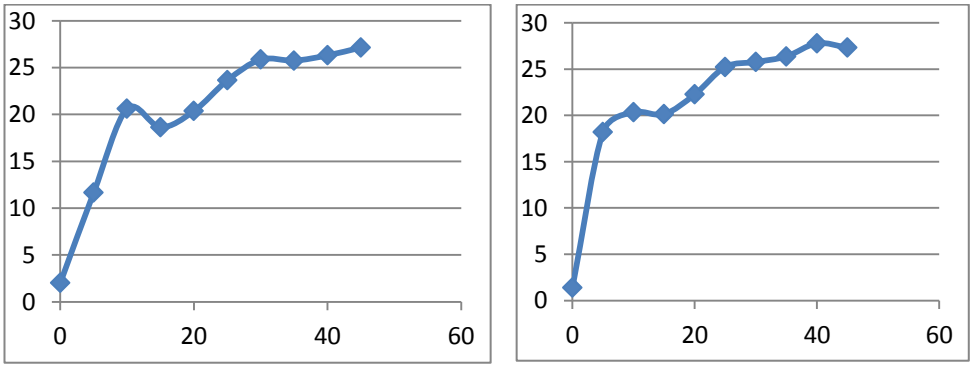

(a) **(b)**

Figure 5.20: TGS 2602 sensor response to PCA algorithm, (a) 1 cigarette test and (b) 2 cigarette test.

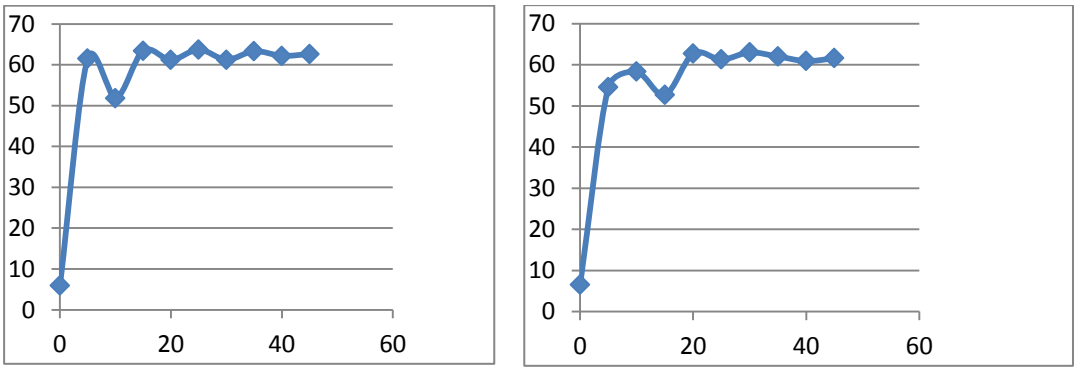

(a) **(b)**

Figure 5.21: TGS 2600 sensor response to PCA algorithm, (a) 1 cigarette test and (b) 2 cigarette test.

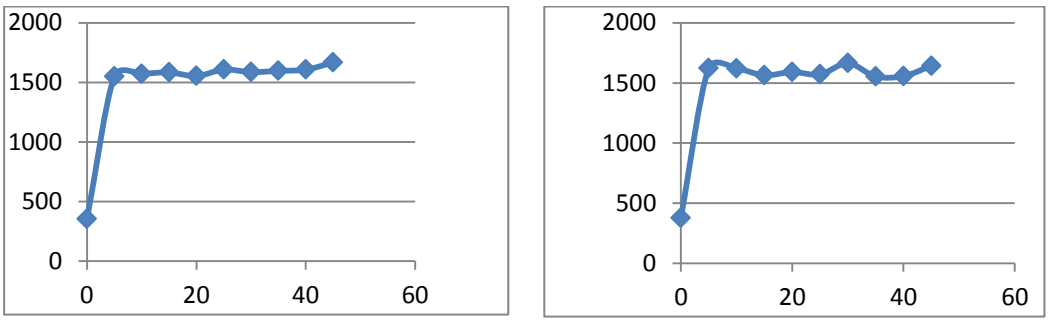

(a) **(b)**

Figure 5.22: TGS 2620 sensor response to PCA algorithm, (a) 1 cigarette test and (b) 2 cigarette test.

We plot three graphs of each sensor, and then we study their performance and similarity, and reach the conclusion about utilization of each algorithm and sensor.

5.5.1 Comparing test graphs by datasheet graphs:

In Graphs of datasheets by decreasing R_s/R_o concentrations of gasses are increasing, so the graphs shapes are descending. Since in test, graphs one axis shows the concentration of gases and the second axes shows the increasing cigarette bighting time or adding the times of spraying ethanol (not R_s/R_o value) our graphs will be ascending. The important point is the similarity and complete agreement between datasheet graphs and the value that system displays in certain concentration of gasses.

5.6 Conclusion and Recommendation

Some conclusion can be achieved by studying graphs, in KNN algorithm, error is a minimum value. This algorithms performance is high. Optimization of codes causes the important disadvantage of KNN algorithm, (time-consuming attributes) be solved. MLP algorithm gives more errors, but errors are in acceptable range. PCA algorithm is used when the input matrix is too large. By applying PCA algorithm to input matrix, the size of matrix will be diminished. In this work, because input data size is not too large, productivity and efficiency of the algorithm is not interesting.

Papers and literature has been reviewed in chapter two. As mentioned in Chapter 2 lots of work has been done on the detection of gases and odors. New technology has given us the possibility to use more advanced sensors. Lots of work has been done before by using PC. Remarkable point in this thesis, which distinguishes it from others, is embedded implementation of three complex algorithms on system that gives capability of being portable. This point gives possibility to use system in robot technologies. This kind of robots can be used in sensitive places like refinery or airports to detect any odor or gas leakage. Using the newest core processing of arm cortex M4 family with the help of its DSP and FPU peripherals that enables us to implement complex processing arithmetic and algorithms in the shortest possible time is other significant point in this thesis. This point enables us to implement algorithms in 1 second, which it could be considered as high speed. As mentioned applying three important algorithms on embedded system is principle point in this work that consumes most of energy and time. The algorithm's nature always gives possibility to predict subsequent value and then uses it as feedback to decreasing error. So it can be concluded that algorithms are used in sensitive and delicate cases. The application that is used for algorithms in this thesis was distinguishing the exact value of gas by PPM scale (that is achieved by training system).

Different applications could be defined for this system. For instance databases of various gases could be given to system and then trained system by written algorithms and new database. Finally by trace dates, system could be able to distinguish between various gases. Many other applications can be defined for algorithms that it depends on other student's creativity and intelligence.

REFERENCES

[1] **Gutierrez-Osuna, R.**(2002) Pattern analysis for machine olfaction: *A review* . *IEEE Sensors Journal, 2(3): 189–202.*

[2] **K. Arshak, G. Lyons, L. Cavanagh, and S. Clifford**.(2003).Front-end signal conditioning used for resistance-based sensors in electronic nose systems*:* A review. Sensor Review, 23(3):230–241.

[3] **Chouhan , R**.(2004) A review of chemical sensors for electronic nose applications. MT&M-Manufacturing Technology and Management, 12(1-2):7–9.

[4] **Pearce,T. C.& Schiffman, S. S., Nagle, H.T.& Gardner**. **J.W.** Handbook of Machine Olfaction.

[5] **Bear, F. , Connors, B. & Paradiso**,**M.**(1986) .Neuroscience Exploring the Brain. William and Wilkins, Baltimore, USA.

[6] **Loutfi, Amy**. Odour Recognition using Electronic Noses in Robotic and Intelligent Systems.

[7] **Ohloff, G**. (1994).Scent and Fragrances. Springer-Verlag, Berlin, UK.

[8] **Wenzel, B.**(1973).Chemoreception. In E. Carterette and M. Friedman, editors, Handbook of Perception, Volume III: Biology of perceptual systems. Academic Press, New York.

[9] **Gesteland, R., Lettvin, J., Pitts, W., and Rojas**, **A.** (1963).Odor specificities of the m frog's olfactory receptors. In Y. Zotterman, editor, Olfaction and Taste. Pergamon, New York.

[10] **Zwaardemaker , H. and Hogewind, F.**(1920).On spray- electricity and waterfall- electricity. Proc. Academic Sci., 22:429–437.

[11] **Seiyama, T., Kato, A., Fujishi, K. and Nagatami**. **M.** (1962).A new detector for gaseous components using semiconductive thin films. Anal. Chem., 32:1502– 1503.

[12] **Wilkens, W. and J. Hartman**. (1972).An electronic analogue for the olfactory process *Acad.* Sci., 116:608–612, 1964.

[13] **Taguchi**. **N.** U.S. Patent 3 695 848.

[14] **Figaro Gas Sensor**: (1992.)Technical Reference, http://www.figaro.com.

[15] **Persaud, K. and Dodd**. **G.** (1982). Analysis of discrimination mechanisms of the mamalian olfactory system using a model nose. Nature, 299:352–355,

[16] **Gardner, J**.(1988.) Pattern recognition in the warwick electronic nose. *In 8th Internationa Congress of European Chemoreception Reasearch Organization*, page 9, Coventry, UK.

[18] **Gardner, J. and Bartlett**, **P.** (1994).A brief history of electronic noses. Sensors and Actuators B, 18,

[19] **Dubois, D. (**2000).Categories as acts of meaning: The case of categories in olfaction and audition. *Cognitive Science Quaterly*, 1:35–68.

[20] **H. Zwaardemaker and F. Hogewind**.(1920) On spray- electricity and waterfall- electricity. Proc. Academic Sci., 22:429–437, [21] **T. Seiyama, A. Kato, K. Fujishi, andM. Nagatami**. A new detector for gaseous components using semiconductive thin films. Anal. Chem., 32:1502– 1503, 1962.

[22] **Wilkens, W. and Hartman, J.**(1964). An electronic analogue for the olfactory process. Acad. Sci., 116:608–612,

[23] **Persaud, K. and Dodd**, **G.** (1982). Analysis of discrimination mechanisms of the mamalian olfactory system using a model nose. Nature, 299:352–355,

[24] **Gardner J**. Pattern recognition in the warwick electronic nose. *In 8th International Congress of European Chemoreception Reasearch Organization*, page 9, Coventry, UK, 1988.

[26] **Branca, A. Simonian, P., M. Ferrante, M., Novas, E. and Negri**, **R.** (2003)Electronic nose. based discrimination of a perfumery compound in a fragrance. Sensors and Actuators *B (*Chemical), B92(1-2):222– 227.

[27] **Fiorillo, S. , Di Bortolomeo, S., Nannini, C. and De Rossi**. **D.(** 1992). Thin layers grown onto copper salt replica for sesor array fabrication. Sensors and Actuato rs-B Chemical, 7:399–403.

[28] **Diego L. García-González and Ramón Aparicio .**Sensors: From Biosensors to the Electronic Nose, Instituto de la Grasa Avda. Padre García Tejero, 41012 Sevilla Spain

[29] **Lundstr¨om, I. , Hedborg, E. Spetz, A. , Sundgren, H. and F. Winquist**. (1992).*Electronic nose based on field effect structures*. In J. Gardner and P. Bartlett, editors, Sensors and sensory systems for an electronic nose, volume 212, pages 303–319, Kluwer, Dordrecht.

[30] **Jones, E.**(1991)The pellistor catalytic gas detector. In P Moseley, J. Morris, and D. Williams, editors, Techniques and mechanism in gas sensing, pages 17–31, Bristol.

[31] **Seitz**, **W.**Chemical sensors based on fiber optics. Anal. Chemistry, 56:16–34, 1984.

[32] **Alpha M.O.S Multi Organoleptic Systems**. (January 2006). Toulouse (France). http://www.alpha-mos.com

[33] **Applied Sensor**,(January 2006). Link¨oping (Sweden), formely MoTech, Reutlingen (Germany). http://www.appliedsensor.com.

[34] **Russell**, **R.**(1999*)* Odour Detection by Mobile Robots. *World Scientific Publishing Co,* London, UK.

[35] **Grate, J., Martin, S. and White**, **R.**(1993). Acoustic wave microsensors, part i. Anal. Chemistry, 64:940–948.

[37] **Gardner, J. and Bartlett, P.**(1999) Electronic Noses, Principles and Applications. Oxford University Press, New York, NY, USA.

[38] **Esbensen, K. , Schonkopf, S. and Midtgaard**, **T.**(1994)Multivariate Analysis in Practice. Camo, Trondheim.

[39] **Jang**, **Roger.** Principal Component Analysis

[40] **Smith , I.** (Web) - A Tutorial on Principle Component Analysis by Lindsay (Cornell University)

[41] **Welling, Max**. Fisher Linear Discriminate Analysis, Department of Computer Science University of Toronto 10 King's College Road Toronto, M5S 3G5 Canada

[42] **Gutierrez-Osuna**, **R.** (1998)"Signal Processing and Pattern Recognition for an Electronic Nose," Ph.D., North Carolina State Univ.

[43] **Harianto, Rivai, Mohammad and Purwanto ,Djoko Purwanto(***1998***)** Implementation of Electronic Nose in Omni-directional , *Department of Electrical Engineering, Institute Teknologi Sepuluh Nopember (ITS) Nose," Ph.D., North Carolina State Univ.*

[44] **Harianto, Robot, Rivai, Mohammad . and Purwanto, Djoko** .Classification of milk by means of an electronic nose and SVM neural network K.

[45] **Blatt , Rossella and Bonarini, Andrea and Calabr´o, Elisa and Matteucci, Matteo and Torre , Della and Pastorino, Ugo**. Classificatio Techniques for Early Lung Cancer Diagnosis using an Electronic Nose

[46] **Gutierrez-Osuna, Ricardo.** Member, IEE .Pattern Analysis for Machine Olfaction: A Review,

[47] **k-Nearest-Neighbors**, www.statsoft.com/Textbook/k-Nearest-Neighbors

[48] **Pan, Leilei and Yang**, **Simon X,** An Electronic Nose Network System for Online Monitoring of Livestock Farm Odors

[49] **Gutierrez-Osuna, Ricardo and Troy Nagle, H.** A Method for Evaluating Data-
Preprocessing Techniques for Odor Classification with an Array of Gas Sensor

[50] **Demuth, Howard and Beale**, Neural Network Toolbox For Use with *MATLAB*®

[51] http://www.mathworks.com/products/neural-network/

[52] STM32F407xx Datasheet, ARM Cortex-M4 32b MCU+FPU, 210DMIPS, up to 1MB Flash/192+4KB RAM, USB OTG HS/FS, Ethernet, 17 TIMs, 3 ADCs, 15 comm. interfaces & caera

[53] RM0090 , Reference manual, STM32F40x, STM32F41x, STM32F4 STM32F43x advanced ARM-based 32-bit MCUs

[54] **Brown, Geoffrey** , Discovering the STM32 Microcontroller, January 8, 2013.

[55] User Manual STM32F4DISCOVERY**,** STM32F4 high-performance discovery Board, www.st.com.

[56] STM32F4DISCOVERY , STM32F4 high-performance discovery board, www.st.com

[57] **Silica Tour,** STM32F4xx Technical Overview, www.emcu.it

[58] http://www.keil.com/arm/mdk.asp

[59] KEIL by ARM, Getting Started For 8-bit, 16-bit, and 32-bit Microcontrollers Creating Applications with µVision®4, /www.keil.com/

APPENDICES

APPENDIX A: STM32F407 block Diagram

APPENDIX B: Sensors Database Tables

Appendix A

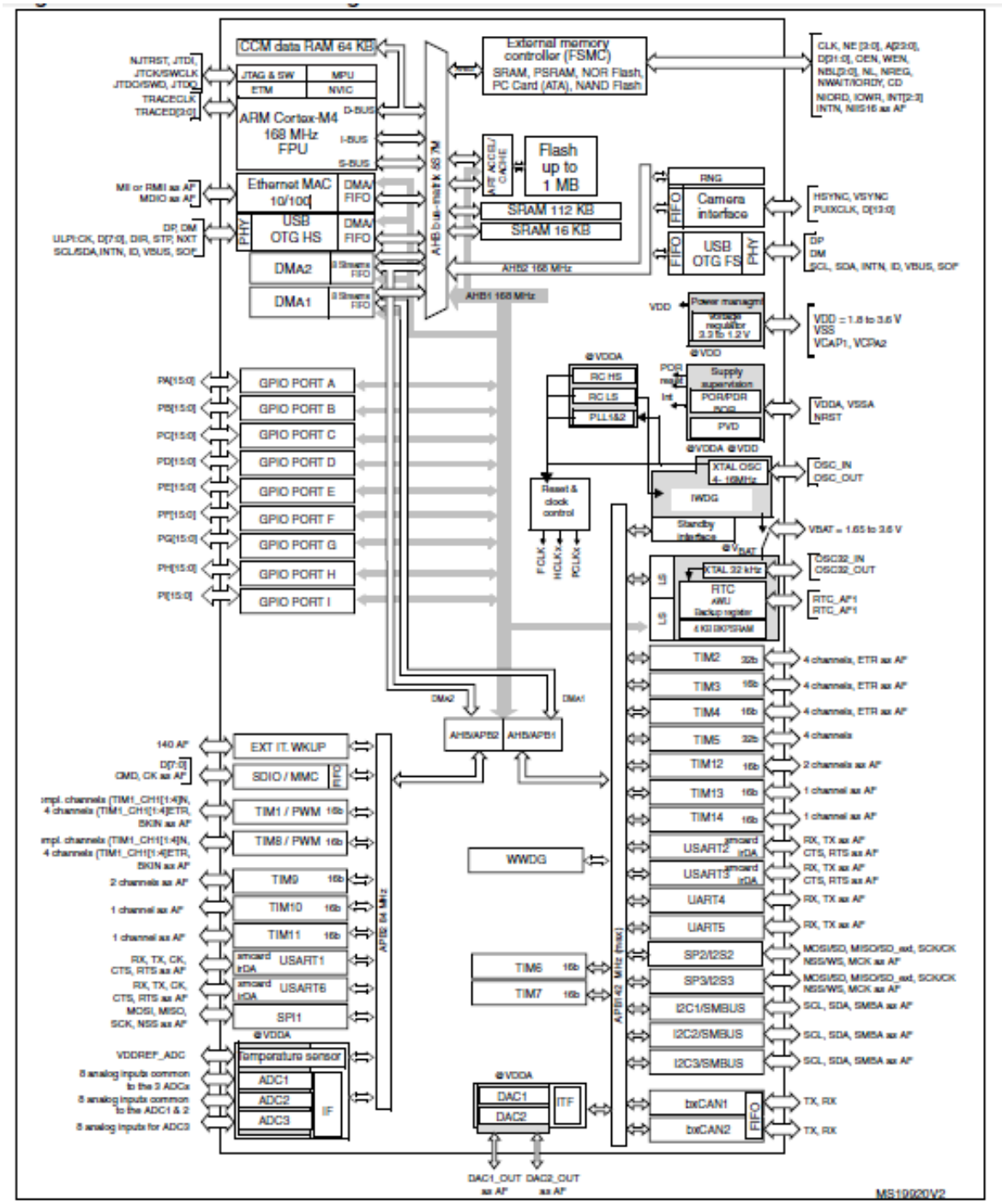
CCM data RAM 64 KB
External memory controller (FSMC)
SRAM, PSRAM, NOR Flash, PC Card (ATA), NAND Flash
JTAG & SW
ETM
MPU
NVIC
ARM Cortex-M4 168 MHz FPU
D-BUS
I-BUS
S-BUS
Flash up to 1 MB
SRAM 112 KB
SRAM 16 KB
Ethernet MAC 10/100
USB OTG HS
USB OTG FS
DMA1
DMA2
RNG
Camera interface
GPIO PORT A
GPIO PORT B
GPIO PORT C
GPIO PORT D
GPIO PORT E
GPIO PORT F
GPIO PORT G
GPIO PORT H
GPIO PORT I
RC HS
RC LS
PLL1&2
Supply supervision
POR/PDR
PVD
XTAL OSC 4- 16MHz
IWDG
Reset & clock control
Standby interface
XTAL 32 kHz
RTC
AWU
Backup register
4 KB BKPSRAM
TIM2
TIM3
TIM4
TIM5
TIM12
TIM13
TIM14
WWDG
USART1
USART2
USART3
UART4
UART5
SP2/I2S2
SP3/I2S3
I2C1/SMBUS
I2C2/SMBUS
I2C3/SMBUS
SDIO / MMC
TIM1 / PWM
TIM8 / PWM
TIM9
TIM10
TIM11
SPI1
TIM6
TIM7
Temperature sensor
ADC1
ADC2
ADC3
DAC1
DAC2
bxCAN1
bxCAN2
AHB1 168 MHz
AHB2 168 MHz
APB1 42 MHz (max)
APB2 84 MHz
MS19920V2

Appendix B

Sensor TGS 2610

Table 5.1: TGS 2610 sensor database in gas concentration

Ethanol	
Rs/Ro	Gas concentration
6	300
5	400
4.7	500
4.3	600
4	700
3.9	800
3.7	900
3.5	1000
2.5	2000
2	3000
1.8	4000
1.5	5000
1.4	6000
1.3	7000
1.2	8000
1.1	9000
1	10000

Table 5.2: TGS 2610 database In air

air	
Rs/Ro	Gas concentration
11	200
11	1000
11	10000
11	11000

Sensor TGS 2602

Table5.3: TGS 2602 sensor database in air

air	Rs/Ro	1	1	1	1
	Gas concentration	0.1	1	10	100

Table5.4: TGS 2602 sensor database in gas concentration

Ethanol	Rs/Ro	0.78	0.6	0.51	0.45	0.41	0.39	0.37	0.35	0.32	0.3	0.2	0.175
	Gas concentration	1	2	3	4	5	6	7	8	9	10	20	30

Sensor TGS 2600

Table 5.5: TGS 2600 sensor database in gas concentration

Ethanol	
Rs/Ro	Gas concentration
1	0.7
2	0.55
3	0.48
4	0.43
5	0.4
6	0.39
7	0.37
8	0.35
9	0.34
10	0.32
20	0.265
30	0.25
40	0.225
50	0.2
60	0.19
70	0.18
80	0.175
90	0.17
100	0.168

Table 5.6: TGS 2600 sensor database in air

air	
Rs/Ro	Gas concentration
1	1
1	10
1	100

Sensor TGS 2620

Table 5.7 : TGS 2620 sensor database in air

Air	
Rs/Ro	Gas concentration
11	50
11	60
11	70
11	80
11	90
11	100
11	200
11	300
11	400
11	500
11	600
11	700
11	800
11	900
11	1000
11	2000
11	3000
11	4000
11	5000

Table 5.8: TGS 2620 sensor database in gas

Ethanol	
Rs/Ro	Gas concentration
3.8	50
3.1	60
2.85	70
2.5	80
2.3	90
2	100
1.35	200
1	300
0.85	400
0.73	500
0.55	600
0.5	700
0.45	800
0.4	900
0.39	1000
0.2	2000
0.15	3000
0.1	4000
0.085	5000

CURRICULUM VITAE

Name Surname: Leila Ghorbani

Place and Date of Birth: Iran-12.01.1986

Address: Iran

E-Mail: leilaghorbani1@yahoo.com

B.Sc.: Electric Electronic Engineering